ABC Transporter-Mediated Transport of Glutathione Conjugates Enhances Seed Yield and Quality in Chickpea[1]

Udita Basu,[a,2] Hari D. Upadhyaya,[b,2] Rishi Srivastava,[a,2] Anurag Daware,[a,2] Naveen Malik,[a,2] Akash Sharma,[a] Deepak Bajaj,[a] Laxmi Narnoliya,[a] Virevol Thakro,[a] Alice Kujur,[a] Shailesh Tripathi,[c] Chellapilla Bharadwaj,[c] V.S. Hegde,[c] Ajay K. Pandey,[d] Ashok K. Singh,[c] Akhilesh K. Tyagi,[a,e] and Swarup K. Parida[a,3,4]

[a]Genomics-assisted Breeding and Crop Improvement Laboratory, National Institute of Plant Genome Research, Aruna Asaf Ali Marg, New Delhi 110067, India
[b]International Crops Research Institute for the Semi-Arid Tropics, Patancheru 502324, Telangana, India
[c]Division of Genetics, Indian Agricultural Research Institute, New Delhi 110012, India
[d]National Agri-Food Biotechnology Institute, Mohali 140306, Punjab, India
[e]Department of Plant Molecular Biology, University of Delhi, South Campus, New Delhi 110021, India

ORCID IDs: 0000-0002-8231-5238 (U.B.); 0000-0002-9079-3205 (A.S.); 0000-0002-1077-7900 (D.B.); 0000-0002-1642-7530 (V.T.); 0000-0001-5142-3781 (S.T.); 0000-0002-9939-3005 (V.S.H.); 0000-0001-7843-3031 (S.K.P.).

The identification of functionally relevant molecular tags is vital for genomics-assisted crop improvement and enhancement of seed yield, quality, and productivity in chickpea (*Cicer arietinum*). The simultaneous improvement of yield/productivity as well as quality traits often requires pyramiding of multiple genes, which remains a major hurdle given various associated epistatic and pleotropic effects. Unfortunately, no single gene that can improve yield/productivity along with quality and other desirable agromorphological traits is known, hampering the genetic enhancement of chickpea. Using a combinatorial genomics-assisted breeding and functional genomics strategy, this study identified natural alleles and haplotypes of an *ABCC3*-type transporter gene that regulates seed weight, an important domestication trait, by transcriptional regulation and modulation of the transport of glutathione conjugates in seeds of *desi* and *kabuli* chickpea. The superior allele/haplotype of this gene introgressed in *desi* and *kabuli* near-isogenic lines enhances the seed weight, yield, productivity, and multiple desirable plant architecture and seed-quality traits without compromising agronomic performance. These salient findings can expedite crop improvement endeavors and the development of nutritionally enriched high-yielding cultivars in chickpea.

The development of nutrient-rich, high-yielding crop cultivars with increased seed size or seed weight (SW) and seed number (SN) is indispensable for ensuring global food and nutritional security. Seed size and SW are among the most vital yield component traits selected during crop domestication, as they not only determine crop yield but also have a huge impact on consumer preference, ultimately influencing the market economics of a crop. Considering the importance of seed size/SW, substantial global efforts have been made to identify genetic factors regulating these vital yield-contributing traits using diverse molecular genetics and functional genomics strategies in crop plants. These efforts have uncovered various signaling pathways, including the brassinosteroid signaling pathway, ubiquitin-proteasome pathway, mitogen-activated protein kinase pathway, G-protein signaling, and a number of transcription factors (TFs) functioning in synchrony to regulate the seed size/SW. These signaling pathways predominantly function through modulation of cell proliferation and cell expansion during seed development (Agarwal et al., 2011; Li and Li, 2015, 2016). Other classes of genes

encoding proteins, such as BIG SEEDS1, histone H4 acetyltransferase, and ATP binding cassette (ABC) transporters, govern the seed size in many monocots and dicots, including *Medicago*, rice (*Oryza sativa*), tomato (*Solanum lycopersicum*), and wheat (*Triticum aestivum*; Orsi and Tanksley, 2009; Song et al., 2015; Walter et al., 2015; Bhati et al., 2016; Ge et al., 2016). However, the regulation of seed size/SW trait variation in *desi* and *kabuli* chickpea (*Cicer arietinum*) remains obscure, ultimately hindering marker-aided genetic improvement of these traits in this important legume crop. Therefore, establishing a comprehensive understanding of the complex genetic architecture of seed size/SW traits is essential for accelerated genetic enhancement of chickpea.

The chickpea, primarily represented by *desi* and *kabuli* cultivars, exhibiting distinct phenotypic variation for diverse agromorphological traits, including pod and seed yield component traits, has been sequenced recently (Jain et al., 2013; Varshney et al., 2013; Parween et al., 2015). Significant efforts involving linkage and association mapping using diverse experimental populations and natural germplasm accessions have been widely deployed to decipher the genetic basis of pod and seed yield trait variation in chickpea. These efforts detected quantitative trait loci (QTLs) and genes associated with multiple pod and seed yield traits, including seed size/SW in chickpea (Kujur et al., 2013, 2015a; Saxena et al., 2014a; Bajaj et al., 2015a; Das et al., 2015a, 2015b; Verma et al., 2015; Singh et al., 2016). However, none of these QTLs/genes are sufficiently robust to regulate seed size/SW across diverse genetic backgrounds and environments, thus hindering marker-assisted genetic improvement of chickpea. Henceforth, efforts to identify robust QTLs/genes regulating seed size/SW in domesticated *Cicer* gene pools and their functional characterization are vital to pave the way for marker-assisted genetic improvement endeavors in chickpea.

This study integrated diverse genome-wide molecular genetics and functional genomics approaches with a genomics-assisted breeding strategy, which led us to delineate an *ABCC3*-type ABC transporter gene that regulates seed size/SW in *desi* and *kabuli* chickpea. The identified ABC transporter gene regulates seed size/SW by modulating glutathione (GSH) conjugate transport in the vacuoles of chickpea seeds. The superior natural alleles/haplotypes of this gene also affect transcriptional activity of its promoter and thus the expression levels of gene haplotypes. These superior molecular signatures scanned from said ABC transporter gene enhanced not only seed size/SW but also other yield and quality component traits in chickpea. Therefore, the identified ABC transporter gene will be an important target for genomic enhancement studies to develop nutritionally enriched, high-yielding *desi* and *kabuli* chickpea cultivars.

RESULTS

Large-Scale Genotyping of Genome-Wide Single Nucleotide Polymorphisms in a Constituted Pod and Seed Yield Trait-Specific Chickpea Association Panel

We constituted a pod/seed yield trait-specific association panel with 291 phenotypically and genotypically diverse accessions encompassing >90% diversity of the global chickpea germplasm lines including international chickpea core collection (ICC) for a genome-wide association study (GWAS; Supplemental Fig. S1). The panel included 189 *desi* and 102 *kabuli* accessions representing 30 diverse ecogeographical regions of the world (Supplemental Table S1).

The paired-end sequencing of 291 accessions using a high-coverage genotyping-by-sequencing (GBS) assay generated ~490 Gb of sequence, with a mean sequencing depth (fold) of 2.3× and 81.6% coverage of the reference *kabuli* genome (Supplemental Fig. S2; Supplemental Table S2). The GBS assay discovered ~5.7 million high-quality single nucleotide polymorphisms (SNPs), of which 83,176 SNPs genotyped in all 291 accessions (association panel) were selected for the GWAS (Supplemental Tables S3 and S4). These SNPs were mapped to eight chromosomes (64,172 SNPs) and unanchored scaffolds (19,004 SNPs) of the chickpea genome with the average frequencies of one SNP per 184.8 kb and 102.7 kb, respectively (Supplemental Fig. S3, A–C). A genome scan plot representing the chromosomal SNP density detected altogether 198 gaps where no SNPs were mapped within 100-kb physical intervals across the chromosomes of the *kabuli* genome (Supplemental Fig. S4; Supplemental Table S5). The 55,127 mined SNPs were annotated on diverse coding and noncoding intronic and regulatory sequence components of 11,803 genes, with the highest proportion (51.3%, 28,284 SNPs) being in the coding DNA sequences (CDS; Supplemental Fig. S3C). A majority of the coding SNPs were nonsynonymous SNPs (53.1%, 15,027 SNPs). The large-effect coding SNPs (863), causing amino acid substitutions and loss or introduction of translation initiation and termination codons, comprised only 3.1% (Supplemental Fig. S3C). The functional annotation identified 2,309 SNPs from 491 TF genes representing 56 TF gene families, of which the highest number of SNPs were in MYB TFs (9.82%; Supplemental Fig. S5). The SNPs detected a higher intraspecific polymorphic potential (189 accessions) belonging to *desi* compared to that of *kabuli* (102 accessions; Supplemental Table S6).

The 64,172 SNPs mapped to chromosomes were employed in phylogenetic tree construction, high-resolution population genetic structure, and principal component analysis (PCA) among 291 *desi* and *kabuli* chickpea accessions belonging to the constituted association panel. This exertion differentiated all these accessions into two distinct populations—68 *kabuli* and 22 *desi* accessions (POP I) and 167 *desi* and 34 *kabuli* accessions (POP II; Fig. 1, A–C). The association panel
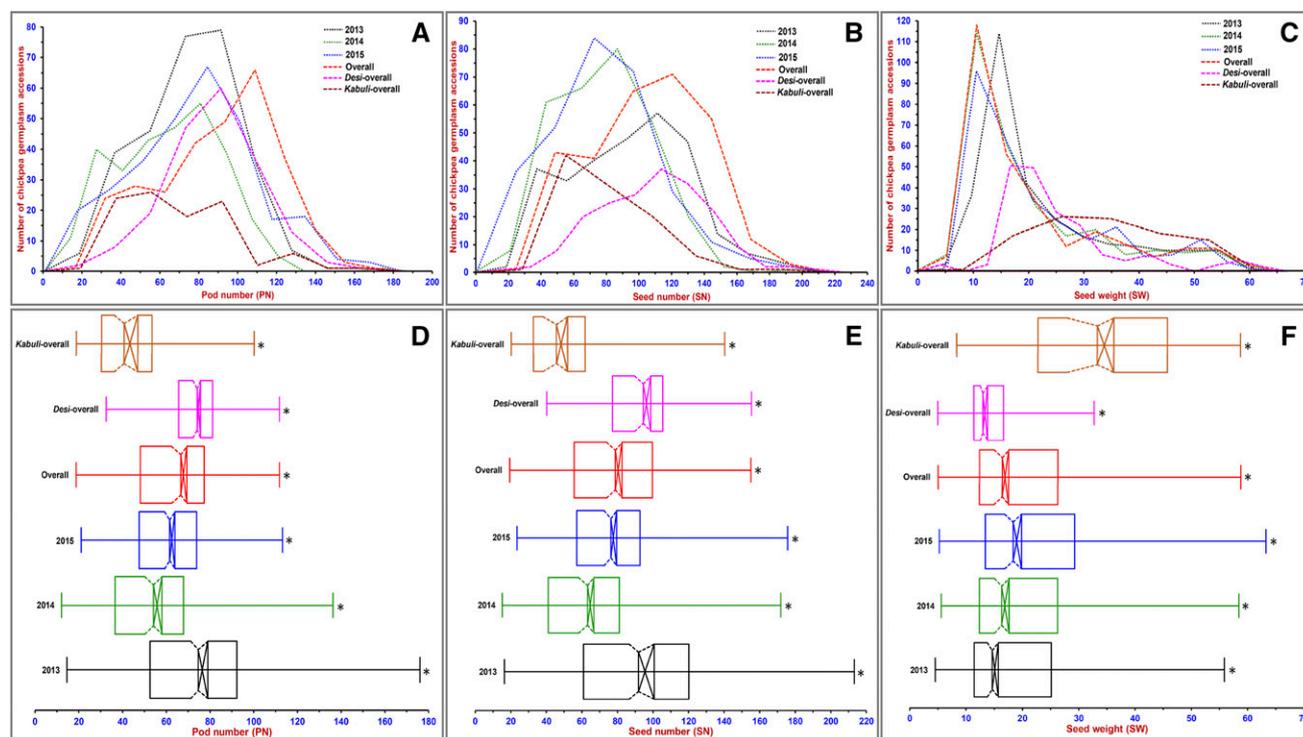
Figure 1. Frequency distribution curves and boxplots depicting the variation in multienvironment (years) field phenotyping data of three major pod/seed yield traits. A–F, PN (A, D), SN (B, E), and 100-SW (C, F), evaluated among the 291 *desi* and *kabuli* accessions (association panel) as a whole and accessions belonging to each *desi* and *kabuli* chickpea cultivar groups. The overall mean of phenotyping information across three environments were also used to generate frequency distribution curves and boxplots. Box edges signify the upper and lower quantiles, with the median value in the middle of the box. *$P < 0.0001$, two-sided Wilcoxon test.

representing a low population structure with extensive phenotypic diversity for pod number (PN), SN, and 100-SW traits had a greater efficiency to detect significant marker-trait association in chickpea, as evident from many earlier GWASs of agronomic traits in crop plants (Supplemental Tables S7 and S8; Kujur et al., 2015a; Yano et al., 2016).

The chromosome-mapped 64,172 SNPs discovered from *kabuli* (0.47 average R^2, 30.2%) vis-à-vis to *desi* accessions detected the highest proportion of linkage disequilibrium (LD) estimates and significant LD ($P <$ 0.0001), with the highest percentage being on the chromosome 4 (Supplemental Table S9). In the whole population, 47.6% SNPs exhibited significant LD and LD estimates (0.41 mean r^2), with the highest being in POP I (Supplemental Table S10). A faster LD decay in POP II (*desi*) than POP I (*kabuli*) at a 200–250-kb physical distance of chromosomes was observed (Fig. 1D). Higher LD estimates and extended LD decay estimated in chickpea compared to that documented in other self- and cross-pollinated crops, such as rice, soybean (*Glycine max*), maize (*Zea mays*), and *Medicago*, was evident (Mather et al., 2007; Lam et al., 2010; Branca et al., 2011; Zhao et al., 2011; Riedelsheimer et al., 2012; Sakiroglu et al., 2012; Xiao et al., 2012). This extended LD decay is expected in chickpea, considering its narrow genetic

base and low intraspecific polymorphism between *desi* and *kabuli* accessions, which might have resulted from the extensive contribution of four successive evolutionary bottlenecks during *Cicer* gene pool domestication (Abbo et al., 2005; Berger et al., 2005; Varma Penmetsa et al., 2016).

GWAS and Regional Association Analysis Scan Potential Genomic Loci in an ABC Transporter Gene Associated with SW in Chickpea

For our GWAS, multienvironment (years) replicated field phenotyping of 291 *desi* and *kabuli* accessions belonging to the association panel was performed for PN, SN, and SW traits in chickpea. We detected a wide variation of said pod and seed yield traits based on their broad coefficient of variation (17.9% to 61.3% CV), as well as high heritability (81% to 89.6% H^2) in the 291 accessions as a whole and between accessions belonging to each *desi* and *kabuli* cultivar group (Fig. 2, A and F; Supplemental Table S7).

The GWAS, by integrating the aforesaid phenotyping and SNP genotyping information of the constituted chickpea association panel based on a compressed mixed linear model (CMLM), detected 14 genomic loci
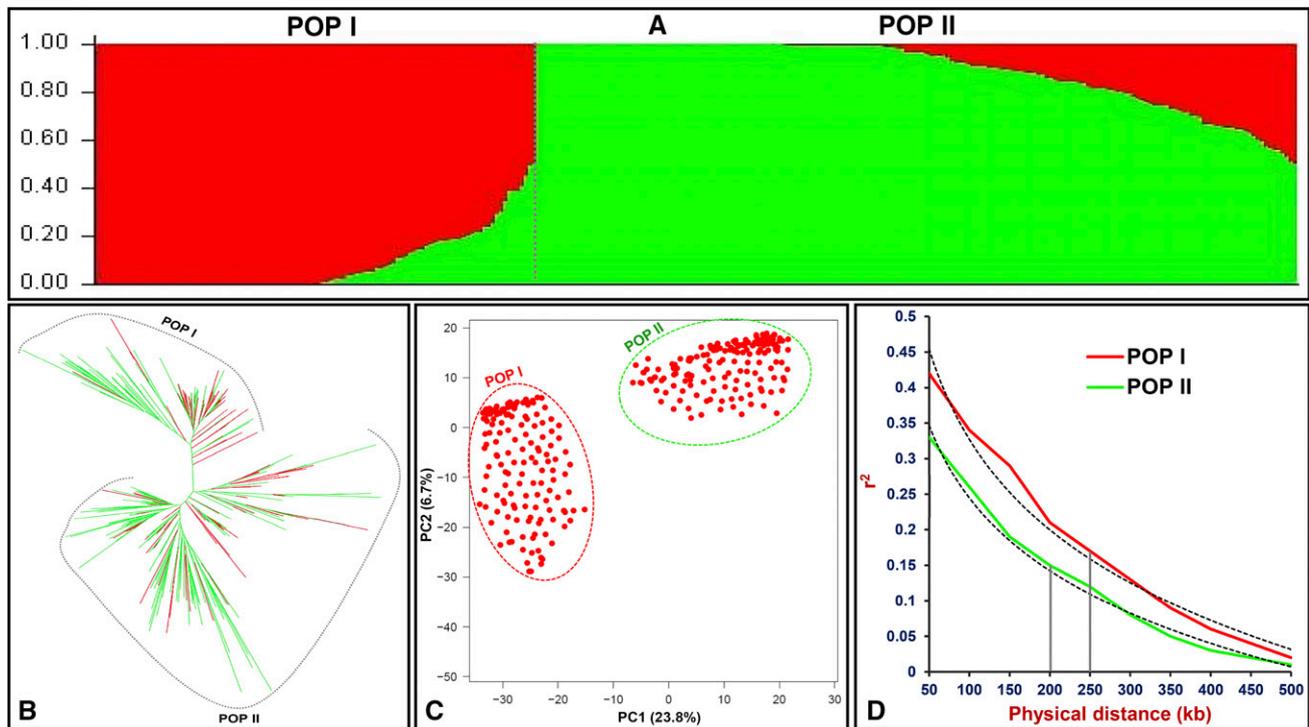
Figure 2. A–D, Determination of molecular diversity, relatedness, and historical recombination (LD) among all 291 *desi* and *kabuli* chickpea accessions (association panel) based on (A) unrooted phylogenetic tree construction, (B) population genetic structure determination, (C) PCA, and (D) LD decay (mean r^2) estimation using 64,172 SNPs physically mapped on chromosomes. These molecular classifications, including population structure (at optimal population number $K = 2$, indicated by red and green colors), differentiated the 291 accessions into two major populations (POP I and POP II). B, In population structure, the accessions represented by vertical bars along the horizontal axis were categorized into K color segments according to their estimated membership fraction in each K cluster. C, In PCA, PC1, and PC2 explained 23.8 and 6.7% of the total variance, respectively. D, In LD decay, the plotted curved lines representing two populations (POP I and POP II) signify the mean r^2 values among SNPs spaced with uniform 50-kb physical intervals from 0 to 500 kb across chromosomes. The dotted lines denote the nonsignificant difference between expected and observed LD decay in the two populations.

exhibiting significant association with PN, SN, and SW traits in at least two of the three environments (Supplemental Fig. S6; Fig. 3). Of these, six genomic loci were associated with PN, SN, and SW traits, whereas two SNP loci exhibited associations with both PN and SW. The remaining six loci associated with SW were validated across all three environments (years), supporting the high heritability of this trait observed in this study (Supplemental Table S11). These trait-associated SNPs were mapped on six chromosomes and further annotated on the coding (synonymous and nonsynonymous) as well as noncoding intronic and regulatory sequence components of 12 genes and intergenic regions of the chickpea genome. The phenotypic variation explained (PVE) by the associated SNPs for PN, SN, and SW traits varied from 10.4% to 33.8% (10^{-5} to 10^{-7} P; Supplemental Table S11). Of these, one synonymous SNP (C-SNP869:A/G) in the CDS of an ABC transporter gene (mapped on chromosome 2) demonstrated a strong association with low (SNP allele "A") and high (SNP allele "G") SW (33.8% PVE, 1.2×10^{-7} probability-value [P]; Figs. 3 and 4A; Supplemental Table S11). The trait association potential of SNPs

determined in the entire population (association panel) remained unaltered with respect to their independent estimation of marker-trait association in *desi* and *kabuli* and the two populations (POP I and POP II).

GWAS-derived candidate genes were further validated through high-resolution targeted sequencing of 250-kb genomic regions (significant LD decay) flanking the 12-SW–associated SNPs in the genes (Supplemental Table S11). For gene-by-gene regional association analysis, the genotyping data of SNPs from the target intervals of associated genes was integrated with multienvironment SW field phenotyping data of all 291 accessions belonging to the association panel (Supplemental Table S12). This delineated a shorter, 430-kb genomic interval (35.10–35.53 Mb with 44 genes) of significant LD resolution (0.83 mean R^2) covering either side of a GWAS-derived SNP (C-SNP869[A/G]) in an ABC transporter gene associated with SW in chickpea (Fig. 4, B and C). Within this LD block, comprehensive gene-by-gene regional association analysis targeting 44 genes detected SNPs from diverse coding (synonymous and nonsynonymous) and noncoding regulatory regions of an ABC transporter
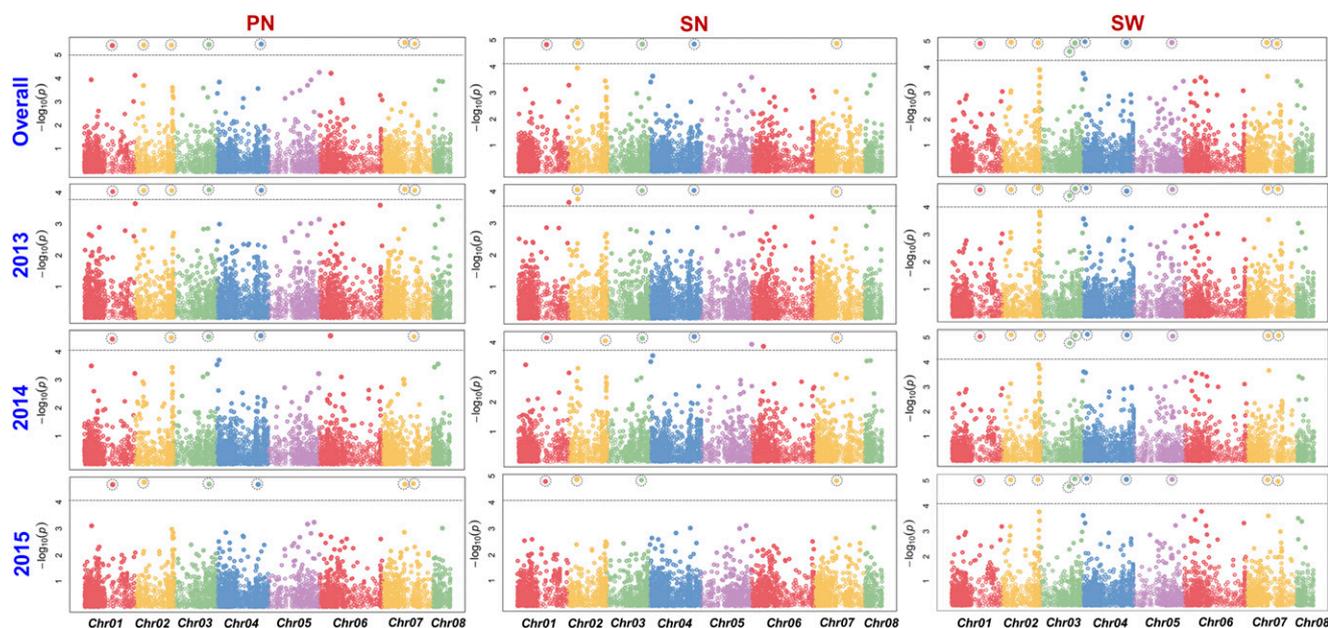
Figure 3. The SNP genotyping and phenotyping information of three major pod/seed yield component traits, PN, SN, and SW, evaluated among 291 *desi* and *kabuli* chickpea accessions were analyzed by environment (year) and using the overall mean across the three environments to generate Manhattan plots. The genomic distribution of SNPs mapped to all eight chromosomes of the *kabuli* genome, is indicated by the x axis. The y axis designates the $-\log_{10}(P)$ value for SNP loci significantly associated with the studied traits. The SNPs exhibiting significant associations with the traits at a cutoff P value $\leq 10^{-4}$ are demarcated with dotted lines. SNPs significantly associated with SW at least in two environments (years) are indicated with black-dotted circles.

gene, demonstrating its strong association potential with SW in chickpea. The implication of the integrated use of a GWAS and high-resolution gene-by-gene regional association analysis for narrowing down a significant trait-associated longer LD block with many candidate genes into a functionally relevant, causal gene is well supported, especially in self-pollinated crop plants (Varshney et al., 2012; Kujur et al., 2015a, 2015b, 2015c; Upadhyaya et al., 2015, 2016; Yano et al., 2016). This integrated strategy is thus useful for effective delineation of potential molecular tags regulating vital agronomic traits in chickpea, in which an extended LD decay (200–250 kb) was observed, especially in the cultivated *Cicer* gene pool.

High-Resolution Molecular Mapping and Map-Based Cloning Reveal an ABC Transporter Gene in a Major QTL Governing SW in Chickpea

To validate the PN-, SN-, and SW-associated genomic loci by molecular mapping of major QTLs, two high-density intraspecific genetic linkage maps of *desi* (ICC 6013 × ICC 14649) and *kabuli* (ICC 13764 × ICC 19192) as well as a consensus high-resolution genetic map were constructed by integrating 9,586, 8,476, and 7,186 SNPs with the average map densities of 0.14, 0.16, and 0.19 centiMorgan (cM), respectively (Supplemental Fig. S7; Supplemental Table S13). A significant phenotypic variation of PN, SN, and SW, based on their broad CV

as well as high H^2 among 282 and 190 individuals and parental accessions of two intraspecific recombinant inbred line (RIL) mapping populations across three environments, was observed (Supplemental Tables S14 and S15). The normal frequency distribution, as well as transgressive segregation of these three major pod and seed yield component traits in two RIL mapping populations of *desi* and *kabuli*, was apparent. High-resolution QTL mapping identified 12 major genomic regions harboring 12 robust (validated across all three environments) QTLs governing PN, SN, and SW mapped to six chromosomes (Supplemental Table S16; Supplemental Fig. S7). The PVE of three studied traits by individual QTL varied from 11.6 to 39.7%, and for all 12 QTLs, it was 35.8%. All 12 SNPs tightly linked to/flanking the 12 major QTLs identified by high-resolution QTL mapping exhibited significant associations with PN, SN, and SW based on our GWAS (Supplemental Tables S11 and S16). Of these, a synonymous SNP (C-SNP869[A/G]) in the CDS of an ABC transporter gene tightly linked to a major *CaqSW2.4* robust QTL revealed strong association with SW based on QTL mapping (39.7% PVE, 17.6 log of odds [LOD]), GWAS (33.8% PVE, 10^{-7} P), and gene-by-gene regional association analysis.

The SW-association potential of this ABC transporter gene was further evaluated through fine-mapping and subsequently by map-based cloning of one strong SW-associated major *CaqSW2.4* robust QTL interval (C-SNP868 [141.4 cM] to C-SNP871 [143.2 cM]) harboring said gene, mapped to two intraspecific RIL
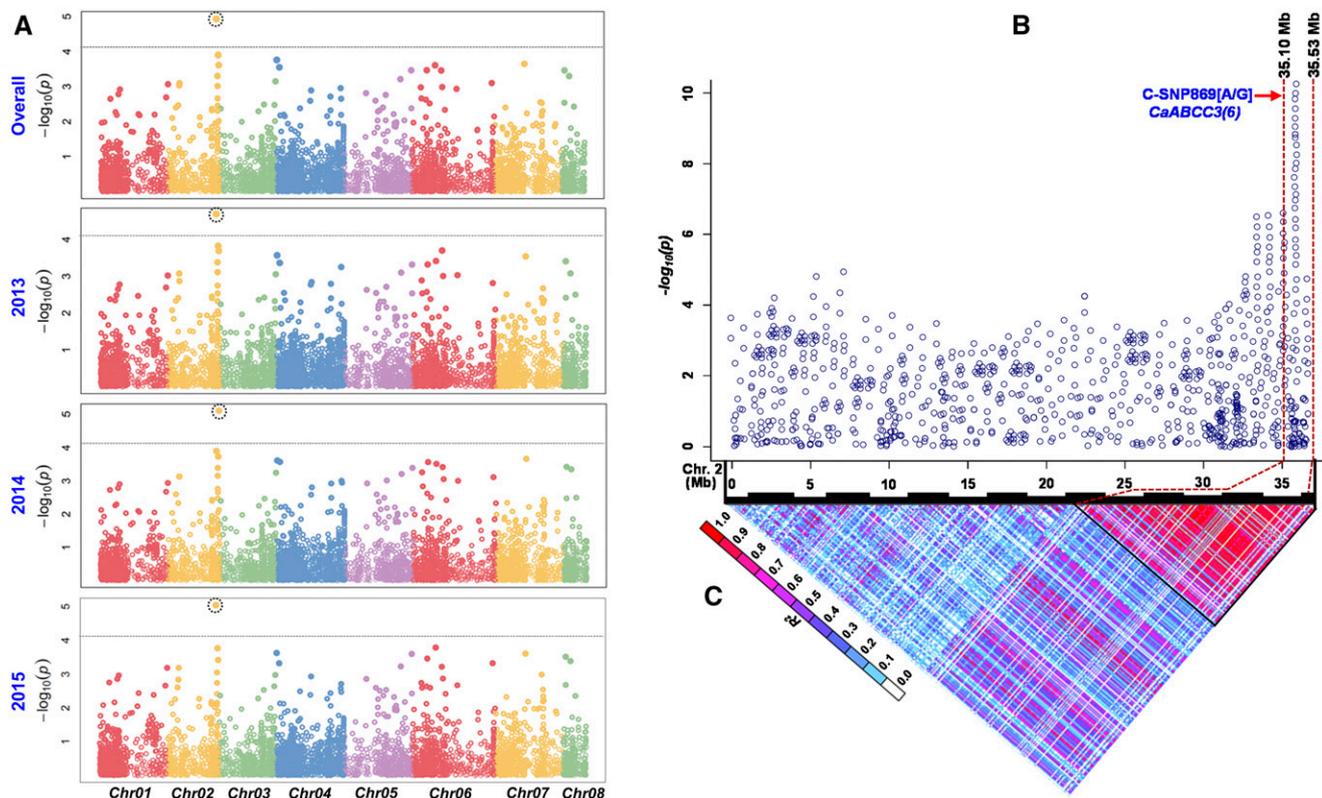
Figure 4. Manhattan plots (A) depicting the significant *P* values of genomic SNP loci associated with 100-SW evaluated among the 291 *desi* and *kabuli* chickpea accessions. The genomic distribution of SNPs mapped on the eight chromosomes of the *kabuli* genome is indicated by the *x* axis. The *y* axis designates the $-\log_{10}$ (*P*) value for SNP loci significantly associated with SW. The SNPs exhibiting significant association with SW at a cutoff *P* value $\leq 10^{-4}$ are demarcated with dotted lines. B and C, Local Manhattan plot (B) and high-resolution LD heat map (C) cover a 430-kb (35.10–35.53 Mb) genomic interval (highlighted with red dotted lines) surrounding a SW-associated significant SNP locus (C-SNP869[A/G]) on chromosome 2. Arrow specifies the genomic position of a trait-associated SNP on chromosome 2. In the LD heat map, r^2 indicates the frequency correlation between pairs of alleles across a pair of SNP loci.

genetic linkage maps (*desi* [ICC 6013 × ICC 14649] and *kabuli* [ICC 13764 × ICC 19192]) and a consensus genetic map (Fig. 5A). This *CaqSW2.4* QTL exhibited a positive additive effect for increasing SW, with a large positive allelic contribution from the high-SW *desi* (ICC 14649) and *kabuli* (ICC 19192) parental accessions. A 437.7-kb major genomic region (C-SNP868 [35,096,032 basepairs (bp)] to C-SNP871 [35,533,752 bp]) underlying a *CaqSW2.4* QTL was defined by integrating its genetic linkage map information with that of the physical map of the *kabuli* chickpea genome (Fig. 5A).

The high-coverage (~120×) multiplex amplicon resequencing of a 437.7-kb *CaqSW2.4* QTL genomic region in parental accessions and 10 of each low- and high-SW homozygous individual from two *desi* and *kabuli* RIL mapping populations altogether detected 301 SNPs. The QTL region-specific association analysis and subsequent high-resolution molecular haplotyping at a *CaqSW2.4* genomic interval by integrating the genotyping information of 301 SNPs with the multi-environment SW phenotyping data among all 291 *desi* and *kabuli* accessions (association panel) were performed. This detected one strong SW-associated

haplotype in the interval between Ca235441704 and Ca235517702 SNPs that scaled down the 437.7-kb *CaqSW2.4* QTL interval into a 76-kb genomic region with 11 protein-coding candidate genes (Fig. 5B).

To further fine-map the *CaqSW2.4* QTL, the 76-kb genomic region between Ca235441704 and Ca235517702 SNPs on chromosome 2 from the donor low- and high-SW *desi* and *kabuli* mapping parental accessions was back-crossed four times into the genetic backgrounds of their corresponding recurrent high- and low-SW parental accessions, to produce four BC_4F_3 near-isogenic lines (NILs), namely, DLSW(ICC 6013-NIL)$^{CaqSW2.4}$, DHSW(ICC 14649-NIL)$^{CaqSW2.4}$, KLSW(ICC 13764-NIL)$^{CaqSW2.4}$, and KHSW(ICC 19192-NIL)$^{CaqSW2.4}$, with ~76% to 81% recovery of the recurrent parental genome (Supplemental Fig. S8, A–D). Using 380 and 277 mapping individuals of two NIL populations of *desi* (DLSW[ICC 6013-NIL]$^{CaqSW2.4}$ × DHSW[ICC 14649-NIL]$^{CaqSW2.4}$) and *kabuli* (KLSW[ICC 13764-NIL]$^{CaqSW2.4}$ × KHSW[ICC 19192-NIL]$^{CaqSW2.4}$), respectively, 79 recombinants were detected between the Ca235442357 (142.4 cM, 35,442,357 bp) and Ca235459613 (143.0 cM, 35,459,613 bp) SNPs at a 17.2-kb *CaqSW2.4* QTL genomic
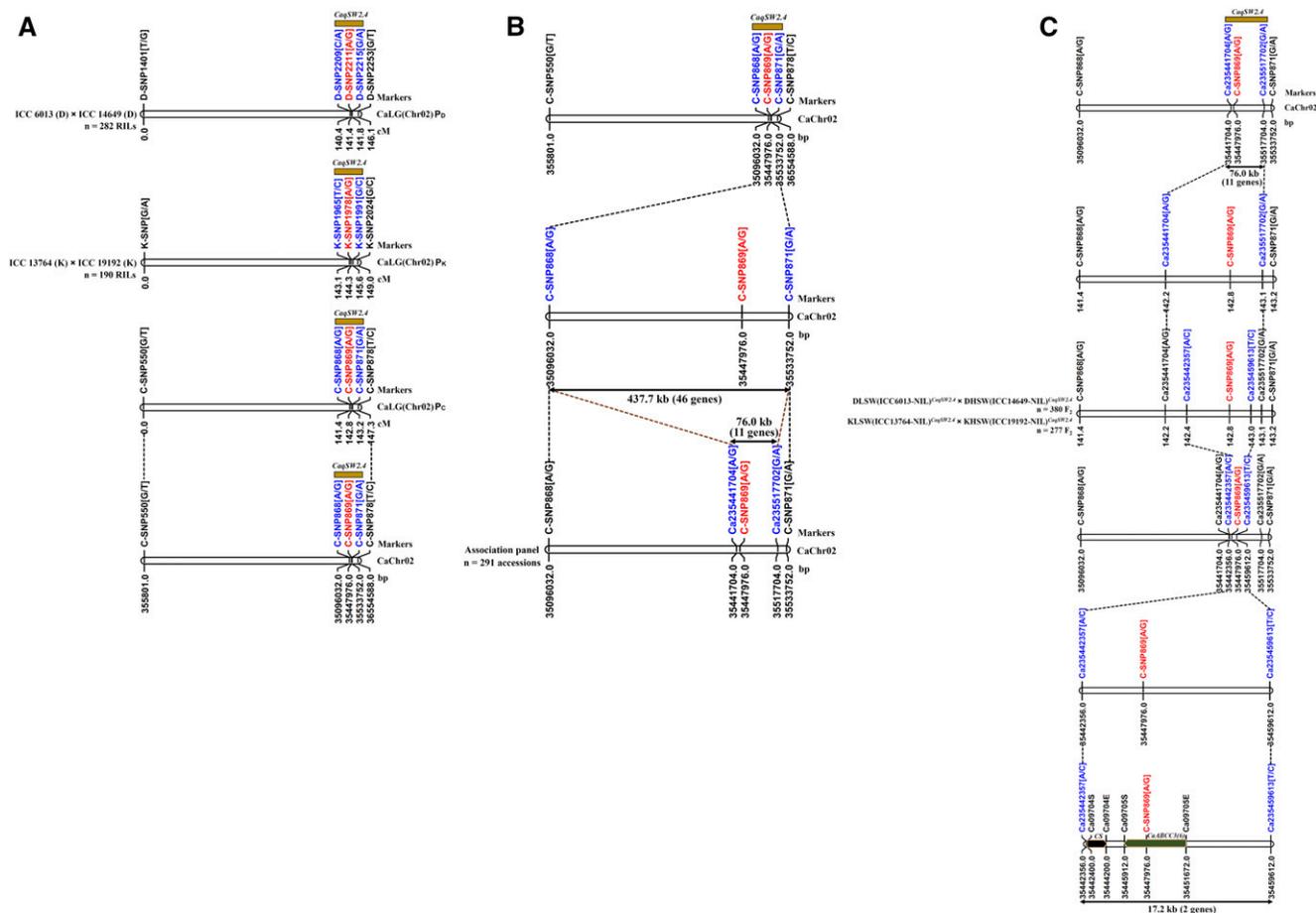
Figure 5. High-resolution molecular mapping and map-based cloning of a major QTL (*CaqSW2.4*) governing 100-SW in chickpea. A, Molecular mapping of a *CaqSW2.4* QTL on chromosome 2 of two high-density intraspecific genetic linkage maps of *desi* (P_D, ICC 6013 × ICC 14649) and *kabuli* (P_K, ICC 13764 × ICC 19192) and on a consensus high-resolution genetic map (P_C) of chickpea. B, The integration of genetic and physical maps of the target genomic region (1.8 cM) harboring a *CaqSW2.4* QTL mapped on a high-density consensus genetic map corresponded to a 437.7-kb sequence interval of chromosome 2. The 437.7-kb *CaqSW2.4* QTL interval was further delimited to a 76-kb sequenced genomic region on chromosome 2 by integrating the aforesaid traditional QTL mapping with QTL region-specific association analysis in the 291 *desi* and *kabuli* accessions belonging to an association panel. C, Fine-mapping of a *CaqSW2.4* QTL using two low- and two high-SW mapping populations of *desi* (380 F2 individuals of DLSW[ICC 6013-NIL]$^{CaqSW2.4}$ × DHSW[ICC 14649-NIL]$^{CaqSW2.4}$) and *kabuli* (277 F2 individuals of KLSW[ICC 13764-NIL]$^{CaqSW2.4}$ × KHSW[ICC 19192-NIL]$^{CaqSW2.4}$) scaled down from the 76-kb QTL interval to a 17.2-kb genomic region with two protein-coding genes, including an ABC transporter *CaABCC3(6)* gene, on chromosome 2. DLSW/KLSW, *Desi/kabuli* low SW; DHSW/KHSW, *Desi/kabuli* high SW.

interval (Fig. 5C). The comprehensive phenotyping of these recombinants after progeny testing resolved a 76-kb *CaqSW2.4* QTL genomic interval into a 17.2-kb region between the Ca235442357 and Ca235459613 SNPs in six selected promising recombinants of the *desi* and *kabuli* NILs (Fig. 6A).

The structural and functional annotation of this 17.2-kb *CaqSW2.4* QTL genomic interval with *kabuli* genome annotation identified two candidate genes: one coding for a cation symporter and one for an ABC transporter, with gene accession IDs Ca_09704 and Ca_09705, respectively (Fig. 6A). One coding synonymous SNP (C-SNP869[A/G]) tightly linked to an ABC transporter gene demonstrated zero recombination with this target locus in the aforesaid six selected recombinants of both

desi and *kabuli* NIL mapping populations. The functionally relevant molecular tags delineated by fine-mapping/map-based cloning were also validated earlier through the GWAS and gene-by-gene regional association analysis and were thus considered the candidate for SW regulation in chickpea.

Transcript Profiling and Molecular Haplotyping Reveal the Role of Natural Alleles and Superior Haplotypes Delineated from an *ABCC3*-type ABC Transporter Gene Modulating SW in Chickpea

The ABC transporter gene delineated within a 17.2-kb *CaqSW2.4* QTL interval showed seed (cotyledon)-specific
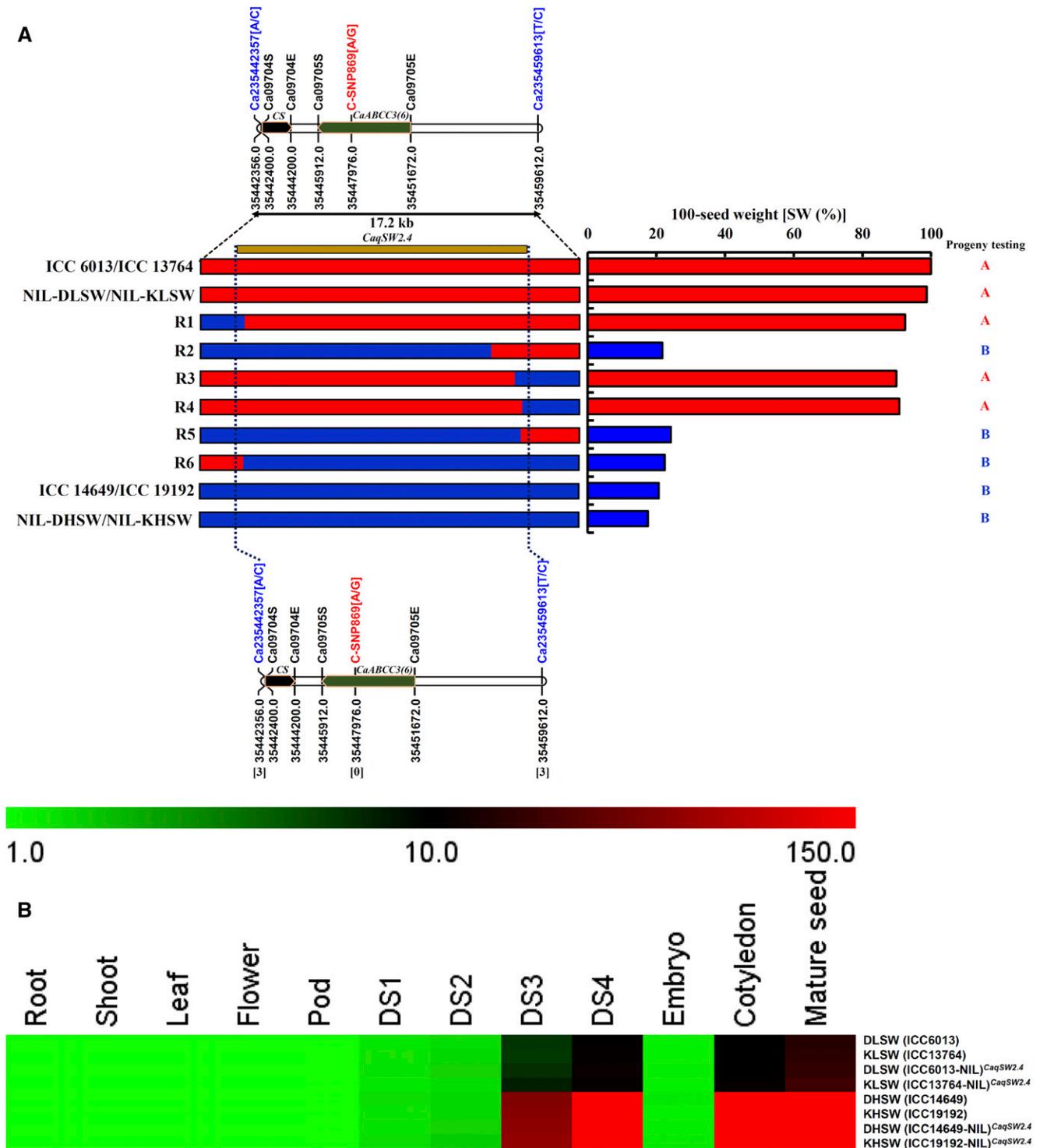
Figure 6. Progeny testing-based individual phenotyping of six selected recombinants as well as low- and high-SW *desi* and *kabuli* NILs and mapping parental accessions to deduce the genotype of a delineated 17.2-kb *CaqSW2.4* QTL governing SW in chickpea (A). Two protein-coding candidate genes annotated within a 17.2-kb *CaqSW2.4* QTL genomic interval between the SNPs Ca235442357(A/C) and Ca235459613(T/C), of which the (C-SNP869[A/G]) synonymous SNP in the coding region of a *CaABCC3(6)* gene, exhibiting zero recombination in selected recombinants, was strongly associated with SW in chickpea. The genomic constitution of low- and high-SW parental accessions/NILs are represented by "A" and "B," respectively. The genetic (cM)/physical (bp) distances and identities of the markers mapped on the LGs/chromosomes are indicated at the left and right sides of the chromosomes, respectively. The SNPs flanking and tightly linked with a *CaqSW2.4* QTL and *CaABCC3(6)* gene mapped on chromosome 2 are indicated with blue and red lines, respectively. The digits inside square brackets denote the numbers of recombinants between *CaqSW2.4* QTL/*CaABCC3(6)* and

expression, which gradually increased with the progression of seed development from stage developmental stage 1 (0–10 days after pollination [DAP]) to DS4 (31–40 DAP; Fig. 6B). The accumulation of transcript of this gene was pronounced (>10-fold) during the later DS3 and DS4 development stages of seeds, as well as in cotyledons and mature seeds, of high-SW (ICC 13764 and ICC 19192) compared to low-SW mapping parental accessions (ICC 6013 and ICC 14649; Fig. 6B). Similar observations were also made in the case of 76-kb *CaqSW2.4* QTL-introgressed NILs of *desi* and *kabuli* chickpea with contrasting SW.

A comprehensive genome-wide survey of ABC transporter genes annotated from the *kabuli* chickpea genome based on characteristics of their encoded domains detected seven different classes (A–G) of 139 ABC transporter genes (Supplemental Fig. S9, A and B; Supplemental Table S17). A strong SW-associated ABC transporter gene delineated by GWAS, gene-by-gene regional association analysis, and map-based cloning was classified as *CaABCC3(6)* in accordance with its orthology with the Arabidopsis *ABCC3* gene (Supplemental Fig. S10, A and B; Supplemental Table S17).

The sequencing followed by molecular haplotyping of the 9761 bp *CaABCC3(6)* gene in all 291 accessions and 81 wild *Cicer* accessions detected 20 SNPs (including five nonsynonymous and nine upstream regulatory SNPs), which altogether constituted three haplotypes (HAP A, HAP B, and HAP C) from each *desi* and *kabuli* and two haplotypes (HAP A and HAP B) in wild chickpea (Supplemental Tables S1 and S18, Fig. 7, A and C). High-resolution gene-specific LD mapping determined through a haplotype pair-based LD estimate produced a significantly high degree of LD (0.87 R^2, $P < 0.0001$) across the entire sequenced regions of the *CaABCC3(6)* gene, thereby increasing its overall potential for SW association in chickpea (Fig. 7D). The haplotype-based association analysis revealed a significant association (41% PVE, 10^{-11} P) of HAP A, HAP B, and HAP C with low, medium, and high SW, respectively. A maximum of 105 and 51 accessions represented by HAP A and HAP C haplotypes in *desi* and *kabuli* exhibited strong association (46% to 47% PVE) with low and high SW, respectively (Fig. 7, E and G). In wild type, both HAP A (44 accessions) and HAP B (37) had comparable trait association potential (42% to 43% PVE) for low and medium SW, respectively.

The *CaABBC3(6)* gene haplotype-specific differential expression profiling assayed through quantitative reverse transcription PCR (RT-PCR) and Northern hybridization demonstrated pronounced expression of the high-SW gene haplotype (HAP C), as expected, especially in later development stages (DS3 and DS4) of seeds, cotyledons, and mature seeds of mapping parental accessions (ICC 14649 and ICC 19192) and corresponding haplotype-introgressed NILs of both *desi* and *kabuli* chickpea with high SW (Fig. 8, A and B). Accordingly, their counterpart low-SW parental accessions (ICC 6013 and ICC 13764) and NILs of *desi* and *kabuli* had reduced accumulation of transcript of the low-SW *CaABCC3(6)* gene haplotype (HAP A).

Functional Validation and Deployment of Natural Alleles and Superior Haplotypes Delineated from an *ABCC3(6)* Gene Regulating SW in Genetic Enhancement of Chickpea

To determine the functional significance of low- (HAP A), medium- (HAP B), and high-(HAP C) SW haplotypes constituted from nine upstream regulatory SNPs of the *CaABCC3(6)* gene on its expression, the molecular basis of differential expression governed by this seed (cotyledon)-specific gene haplotype was deciphered in *desi* and *kabuli* chickpea. Haplotype-specific fragments were amplified from corresponding low- (HAP-A) and high- (HAP C) SW haplotype-introgressed *desi* and *kabuli* NILs and four medium-SW *desi* (ICC 8318 and ICC 12426) and *kabuli* accessions (ICC 7272 and ICC 7654) of chickpea. These fragments were used for a beta-glucuronidase (*GUS*)-transient assay of upstream haplotype gene constructs in agro-infiltrated leaf samples of a high-yielding Indian *desi* variety, ICCV 93954. The transformation efficiency was normalized to a green fluorescent protein (*GFP*) reporter gene cotransfected with the said upstream haplotype *GUS* gene constructs. This revealed a significant difference in the normalized transcript abundance of the *GUS* gene from three haplotype constructs varying in regulatory SNPs, reflecting a positive correlation between SW and transcript accumulation of haplotypes in a selected chickpea accession with similar genetic background (Fig. 8C). This implies differential transcriptional activity of promoter haplotypes constituted from a *CaABCC3(6)* gene, which is one of the major determinants of SW regulation in *desi* and *kabuli* chickpea.

Subcellular localization of low- (HAP-A) and high- (HAP C) SW *CaABCC3(6)* gene haplotypes in normal

Figure 6. (*Continued.*)
SNPs. B, The differential expression profile of *CaABCC3(6)* (validated by high-resolution GWAS, gene-by-gene regional association mapping, and map-based cloning) in vegetative (root, shoot, and leaf) and reproductive (flower, pod, embryo, cotyledon, and mature seed) tissues and four seed development stages (DS1–DS4) of 76 kb *CaqSW2.4* QTL-introgressed NILs as well as mapping parental accessions (ICC 6013, ICC 14649, ICC 13764, and ICC 19192) of *desi* and *kabuli* with low and high SW. The green, black, and red in the color scale at the top signify low, medium, and high average log signal expression of genes in different tissues/stages, respectively. The accessions/NILs and tissues selected for expression profiling are indicated on the right and upper part of the expression map, respectively. DLSW/KLSW, *Desi/kabuli* low SW; DHSW/KHSW, *Desi/kabuli* high SW; and NIL, near-isogenic line. DS1, 0–10 DAP; DS2, 11–20 DAP; DS3, 21–30 DAP; and DS4, 31–40 DAP.
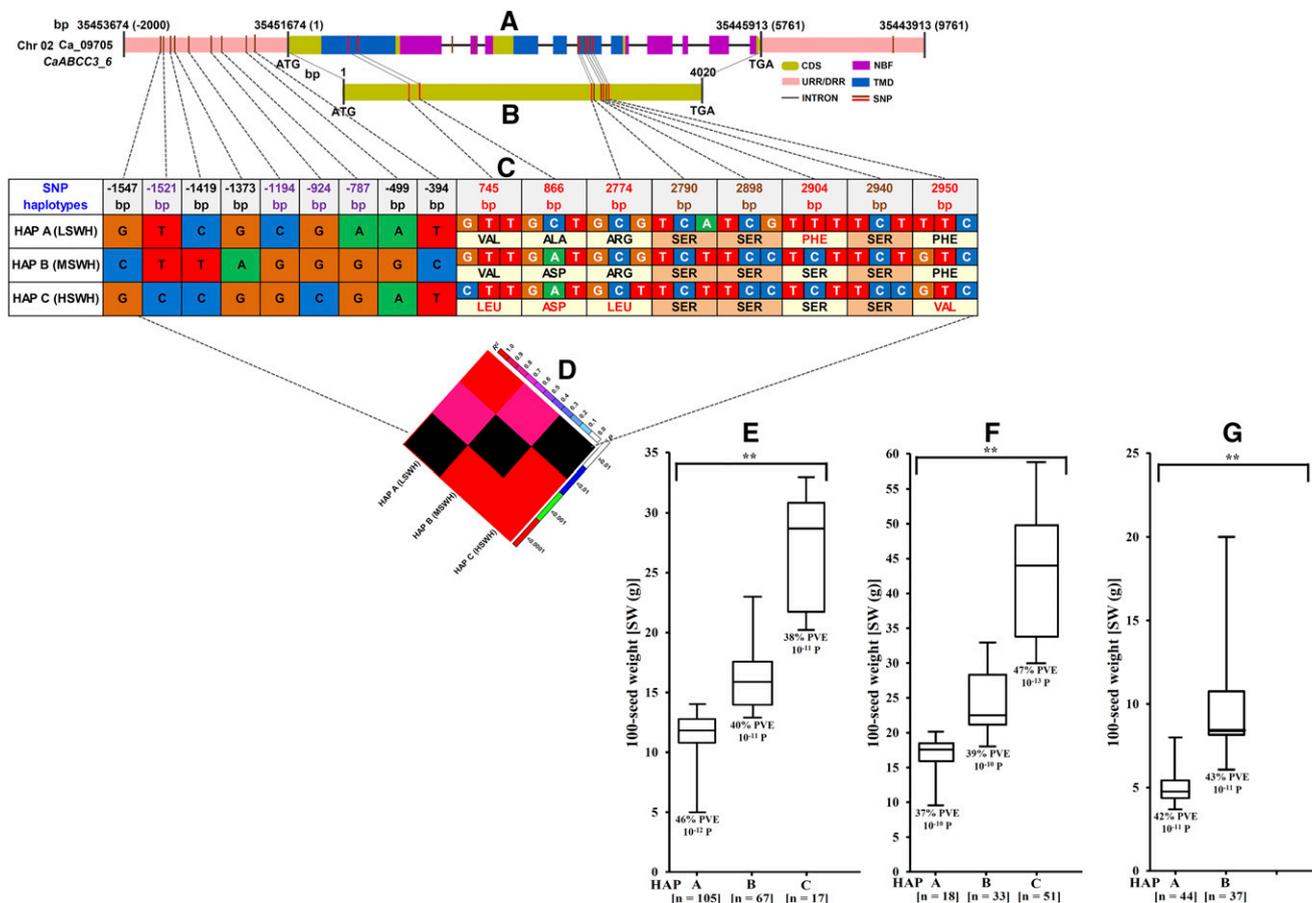
Figure 7. Haplotype-specific LD and association mapping in a strongly SW-associated gene, *CaABCC3*(*6*), delineated by GWAS, gene-by-gene regional association analysis and map-based cloning. Genomic organization/constitution of the *CaABCC3*(*6*) gene (A) including its (B) CDS, exhibiting the distribution of SNPs in different sequence components of this gene. C, The genotyping of 20 SNPs (A and B) in different coding and noncoding sequence components of *CaABCC3*(*6*) in all 291 cultivated (*desi* and *kabuli*) and 81 wild chickpea accessions constituted three haplotypes (D). Three haplotypes, HAP A, HAP B, and HAP C, exhibited strong association with low, medium, and high SW, respectively. The nonsynonymous and regulatory SNPs exhibiting differentiation, especially between LSWH (HAP A) and HSWH (HAP C), are highlighted in red and violet, respectively. The value r^2 indicates the frequency correlation between pairs of alleles across a pair of SNP loci. Boxplots for 100-SW based on three haplotypes, HAP A, HAP B, and HAP C, constituted in (E) *desi* (189 accessions), (F) *kabuli* (102), and (G) wild (81) chickpea, demonstrating their strong associations with low, medium, and high SW, respectively. Box edges represent the upper and lower quantiles, with the median value in the middle of the box. The digits within the square brackets denote the number of accessions representing each class of haplotype associated with SW. *$P < 0.0001$, two-sided Wilcoxon test. HAP, haplotype; LSWH/MSWH/HSWH, low-/medium-/high-SW haplotype.

and plasmolyzed living onion (*Allium cepa*) cells illustrated the predominant colocalization of both of their encoded GFP-fused proteins along with a vacuole-specific marker (vacuolar iron transporter 1 protein) within the vacuole as a bounded membrane (tonoplast)-associated protein.

We constituted desi/kabuli low- (DLSW[ICC 6013-NIL]$^{CaABCC3[6]DLSWH}$ and KLSW[ICC 13764-NIL]$^{CaABCC3[6]KLSWH}$) and high- (DHSW[ICC 14649-NIL]$^{CaABCC3[6]DHSWH}$ and KHSW[ICC 19192-NIL]$^{CaABCC3[6]KHSWH}$) SW NILs of chickpea using haplotype-assisted foreground selection. This was performed by introgression of low- (HAP-A) and high-(HAP C) SW *CaABCC3*(*6*) gene haplotypes along with SNPs linked to/flanking a major *CaqSW2.4* QTL and a

strongly SW-associated *CaABCC3*(*6*) gene. Foreground selection and subsequent 1,536 SNP-based background selection enhanced the recovery of the parental recurrent genome up to 99.1% to 99.6% in the constituted low- and high-SW NILs (Fig. 9A; Supplemental Figs. S8 and S11). This implies greater efficacy and wider practical applicability of gene haplotype-aided selection compared to most commonly used marker-assisted selection (75% to 85%) in the recovery of a parental recurrent genome, as well as precise selection of the most promising recombinants for further genetic enhancement studies not only in chickpea but also in other crop plants.

To know whether *CaABCC3*(*6*) gene haplotypes control SW through maternal and/or zygotic effects, reciprocal F1 crosses using a pair of low- and high-SW
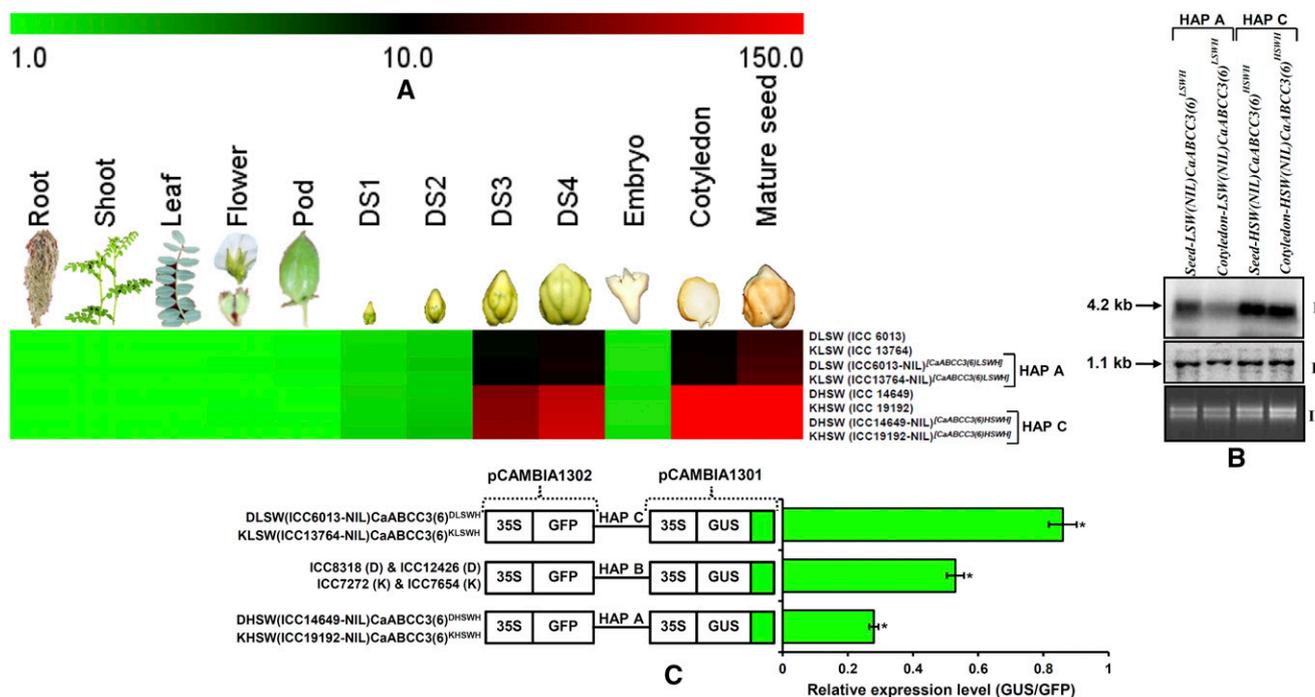
Figure 8. The differential expression profile of low- (HAP A) and high- (HAP C) SW *CaABCC3*(*6*) haplotypes of *desi* and *kabuli* in vegetative (root, shoot, and leaf) and reproductive tissues (flower, pod, embryo, cotyledon, and mature seed) and four seed development stages (DS1–DS4) of corresponding haplotype-introgressed NILs of *desi* and *kabuli* with low and high SW (A). The green, black, and red in the color scale at the top signify low, medium, and high average log signal expression values of the gene in different tissues/stages, respectively. The accessions/NILs and tissues selected for expression profiling are indicated on the right and upper part of the expression map, respectively. B, Autoradiogram depicting the northern hybridization pattern of strongly SW-associated low- (HAP A) and high- (HAP C) SW *CaABCC3*(*6*) haplotypes in seed and cotyledon of corresponding haplotype-introgressed NILs with contrasting SW. The transcript sizes (in kb) hybridizing with the probes. (I) *CaABCC3*[6] gene haplotypes and (II) *elongation factor 1-alpha* as an internal control are indicated by arrows. (III) Normalized RNA isolated from the tissues of NILs. C, Transient expression assay to determine the effects of low- (HAP A), medium- (HAP B), and high- (HAP C) SW haplotypes of *desi* and *kabuli* constituted by the regulatory SNPs from the URR of *CaABCC3*(*6*) on its expression. Left, the construct backbone with URR haplotypes (HAP A, HAP B, and HAP C) of *desi* and *kabuli* influencing the expression of the cauliflower mosaic virus (*CaMV*) 35S promoter-driven *GUS* (β-glucuronidase) reporter gene (cloned in pCAMBIA1301) along with a control *CaMV* 35S promoter regulating the expression of the GFP (*GFP*) reporter gene (cloned in pCAMBIA1302). Right, corresponding expression levels of *GUS*-URR haplotypes relative to control *GFP* in corresponding haplotype-introgressed low- and high-SW NILs of *desi* and *kabuli*. To estimate the effect of the medium-SW haplotype (HAP B) on *CaABCC3*(*6*) gene expression, four *desi* (ICC 8318 and ICC 12426) and *kabuli* accessions (ICC 7272 and ICC 7654) with medium SW were selected from a constituted association panel for a transient expression assay. Horizontal error bars signify the mean SE for each construct with 18 independent replicates. Asterisk (*), Significant difference statistically at a $P \leq 0.0001$ estimated by Duncan's test. DLSW/KLSW, *Desi/kabuli* low SW; DHSW/KHSW, *Desi/kabuli* high SW; LSWH/HSWH, low-/high-SW haplotype; and NIL, near-isogenic line.

NILs of *desi* (DLSW[ICC 6013-NIL]$^{CaABCC3[6]DLSWH}$ × DHSW[ICC 14649-NIL]$^{CaABCC3[6]DHSWH}$) and *kabuli* (KLSW[ICC 13764-NIL]$^{CaABCC3[6]KLSWH}$ × KHSW[ICC 19192-NIL]$^{CaABCC3[6]KHSWH}$) were made. A nonsignificant ($P < 0.0001$) variation of SW in reciprocal crosses of the aforesaid NILs and a significant difference in SW between the self-pollinated NILs ($P < 0.001$) was apparent. This reflects that *CaABCC3*(*6*) gene haplotypes control SW solely through the influence of the zygotic effect but not by the genotype of the maternal environment of seeds in chickpea (Supplemental Fig. S12).

The high-SW *CaABCC3*(*6*) gene haplotype (HAP C)-introgressed NILs compared to low-SW (HAP A) NILs of *desi* and *kabuli* chickpea exhibited a significant increase in SW with the progression of seed development

from stage DS2 (1.9-times) to DS4 (4.7), which was reflected in its seed morphometric features observed by a light microscope-based histological assay (Fig. 10A; Supplemental Fig. S13). At a mature stage, the seeds (cotyledons) of high-SW *desi* and *kabuli* NILs were 73.7% higher ($P < 0.0001$) than seeds (embryos) of low-seed-weight NILs. The significant difference in SW between high- and low-SW NILs of *desi* and *kabuli* was because of additive interaction of high- and low-SW alleles/haplotypes in which the predominant genetic effect of high-SW alleles (haplotypes) increased SW by 74% in chickpea. This observation agrees well with the expression pattern of high- (HAP C) and low- (HAP A) SW haplotypes in NILs during seed development (Fig. 8, A and C).
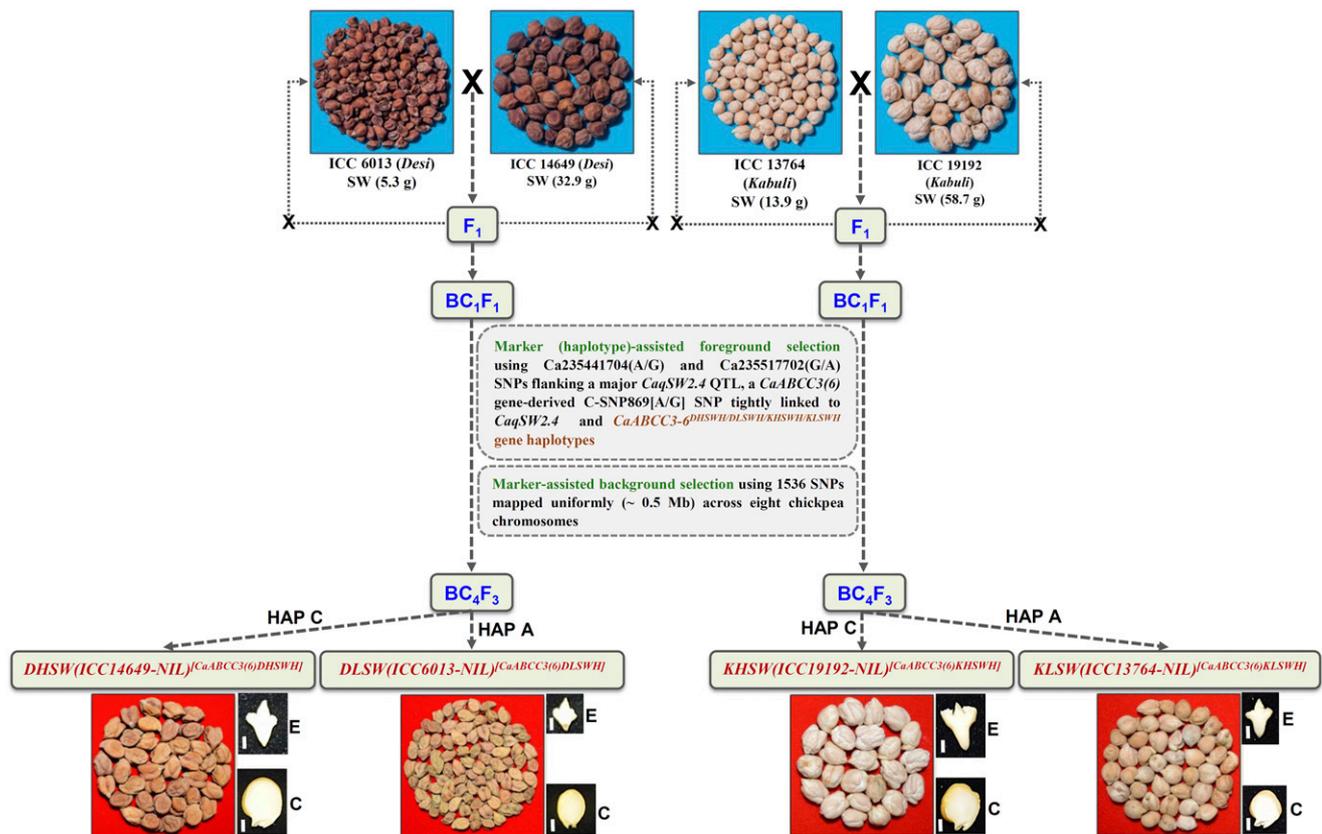
Figure 9. Schematic depiction of the strategies undertaken to develop high- and low-SW NILs of *desi* and *kabuli* chickpea by introgressing the 76-kb *CaqSW2.4* QTL and target trait-specific *CaABCC3(6)* haplotypes from corresponding high- and low-SW parental accessions of two intraspecific mapping populations of *desi* (ICC 6013 × ICC 14649) and *kabuli* (ICC 13764 × ICC 19192) with their counterparts through marker/haplotype-assisted foreground and background selection as depicted in Supplemental Figure S8. DLSW/KLSW, *Desi/kabuli* low SW; DHSW/KHSW, *Desi/kabuli* high SW; NIL, near-isogenic line; DLSWH/DMSWH/DHSWH, *Desi* low-/medium-/high-SW haplotype, respectively; KLSWH/KMSWH/KHSWH, *Kabuli* low-/medium-/high-SW haplotype; E, embryo; C, cotyledon. Scale bar = 1 cm.

The strong SW-associated *CaABCC3(6)* chickpea gene, a homolog of Arabidopsis (*Arabidopsis thaliana*) ATP-dependent multidrug-resistance–associated protein 3/*ABCC3*, can transport GHS s-conjugates (Tommasini et al., 1998; Klein et al., 2006). However, the precise regulatory molecular function of this *ABCC3*-type transporter gene during seed development and SW variation is completely unknown in crop plants, including chickpea. To study the role of the *CaABCC3(6)* gene and its constituted haplotypes in controlling seed development, diverse functional genomics approaches were employed in different development stages/tissues of seeds of high- and low-SW NILs. Given the role of the *CaABCC3(6)* homolog in Arabidopsis in GHS-conjugate transport, total GSH content at developmental stages of seeds (cotyledons and mature seeds) in seed vacuoles of high- (HAP C) and low- (HAP A) SW haplotype-introgressed NILs of *desi* and *kabuli* chickpea was estimated. The accumulation of GSH content increased with the progression of seed development from stage DS2 (1.3-times) to DS4 (1.8) in seeds and cotyledons of high-SW NILs

compared to the low-SW NILs of *desi* and *kabuli* chickpea (Fig. 10B). The expression profiling of five genes known to be involved in metabolism and transport of GS-conjugates in the cell, including cytosol and vacuole, was compared with low- and high-SW *CaABCC3(6)* gene haplotypes. These known genes did not exhibit any differential expression in later development stages of seeds of high- and low-SW NILs (Supplemental Table S19; Supplemental Fig. S14).

The yeast mutant complementation assay suggested that the function of the *CaABCC3(6)* gene was similar to that of the yeast YCF1 and thus could help in GS-conjugate transportation and detoxification (Li et al., 1996; Lu et al., 1998; Tommasini et al., 1998; Bhati et al., 2014, 2015). The high-SW haplotype HAP C efficiently complemented the Δ*ycf1* mutant strain (sensitive for cadmium treatment). However, the low-SW haplotype HAP A was unable to rescue the mutant phenotype, implying its incompetence in performing the transportation of GS-conjugates (Fig. 10C). The loss of transportation ability of the low-SW haplotype HAP A was further corroborated by its decreased
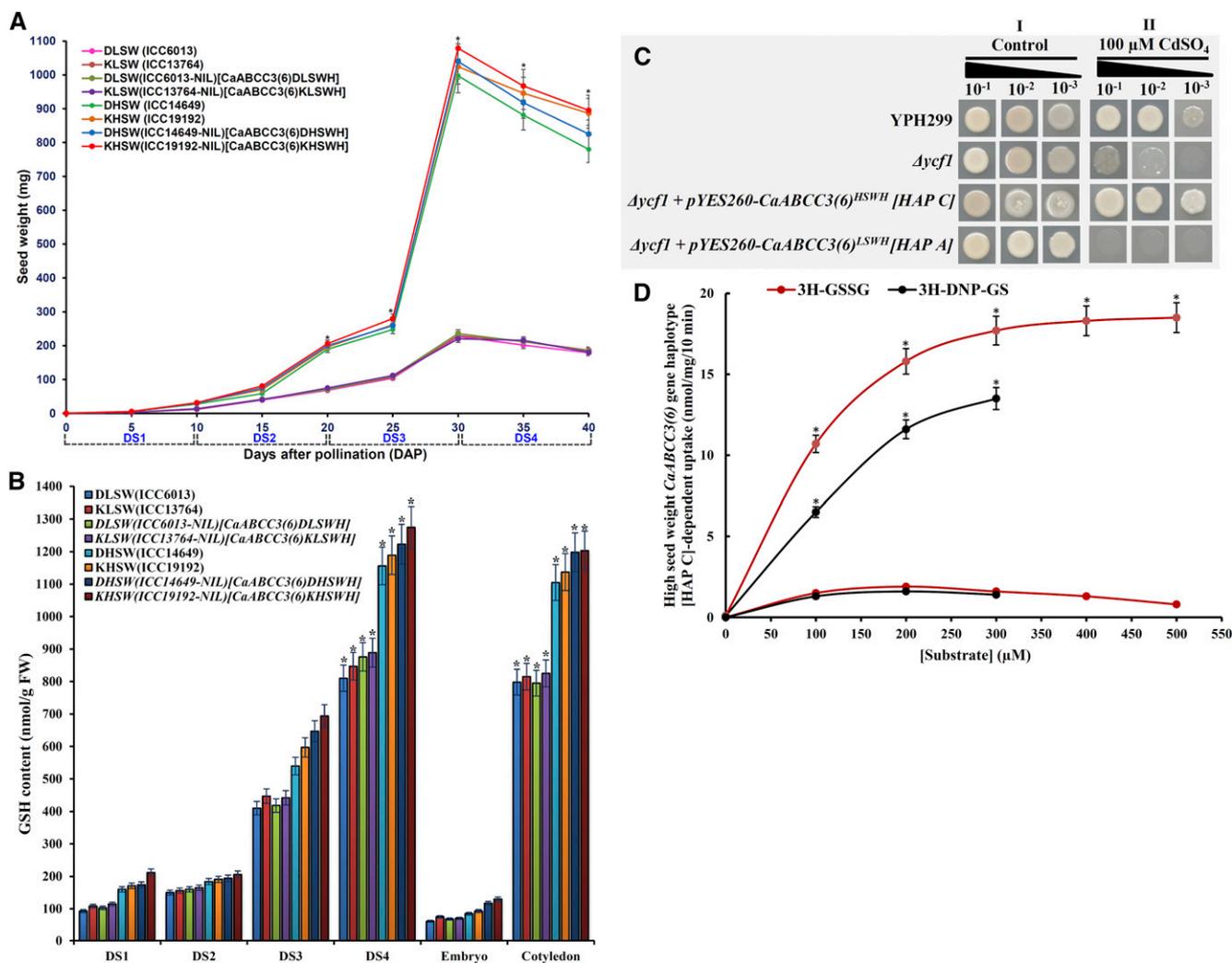
Figure 10. Variation in SW mediated through modulation of GHS content and GHS conjugates transportation during seed development stages of *CaABCC3*(*6*) gene haplotype-introgressed NILs of *desi* and *kabuli* chickpea. A, Physical estimation of variation in average weight (mg) of single seed during development stages (DS1–DS4) of seeds, including embryo and cotyledons of low- and high-SW *desi* and *kabuli* NILs as well as *desi* and *kabuli* mapping parental accessions (ICC 6013, ICC 14649, ICC 13764, and ICC 19192). Error bars represent SE (*n* = 60). *P < 0.001, Student's two-tailed *t* test. B, Variation in GSH content (nmol) measured in one gram fresh weight (FW) of seeds during the development stages (DS1–DS4) of seeds, including embryo and cotyledons of low and high SW *desi* and *kabuli* NILs as well as *desi* and *kabuli* mapping parental accessions (ICC 6013, ICC 14649, ICC 13764, and ICC 19192). Error bars represent SE (*n* = 60). *P < 0.001, Student's two-tailed *t* test. C, Complementation assay of yeast Δ*ycf1* mutants by *CaABCC3*(*6*) gene haplotypes. Yeast parent strain YPH299 and its Δ*ycf1* mutant was used for the complementation of high (HAP C, *CaABCC3*[*6*]^{HSWH}) and low (HAP A, *CaABCC3*[*6*]^{LSWH}) SW haplotypes constituted from a *CaABCC3*(*6*) gene. Empty vector pYES260 transformed to both the strains were used as control. After induction, an aliquot of cells at an optical density of 0.1 and subsequent 10-fold dilutions of the same were spotted on YPD plates containing (I) no $CdSO_4$ as control and (II) 100 μM of $CdSO_4$ and incubated at 30°C. Images of all the plates were captured 3 d post incubation. D, *CaABCC3*(*6*) gene haplotype-dependent uptake of ^{3}H-GSSG and ^{3}H-DNP-GS. The rates of high (HAP C, *CaABCC3*[*6*]^{HSWH}) and low SW *CaABCC3*[*6*] gene haplotype (HAP A, *CaABCC3*[*6*]^{LSWH})-dependent uptake were estimated by subtracting the radioactivity acquired by vacuolar membrane-enriched vesicles prepared from pYES3-transformed cells from that acquired by the equivalent membrane fraction from pYES3-(HAP C, *CaABCC3*[*6*]^{HSWH}) or pYES3-(HAP A, *CaABCC3*[*6*]^{LSWH})-transformed DTY168 cells. Error bars represent SE (*n* = 3). *P < 0.001, Student's two-tailed *t* test. DS1, 0–10 DAP; DS2, 11–20 DAP; DS3, 21–30 DAP; and DS4, 31–40 DAP. DLSW/KLSW, *Desi/kabuli* low SW; DHSW/KHSW, *Desi/kabuli* high SW; DLSWH/DMSWH/DHSWH, *Desi* low-/medium-/high-SW haplotype; KLSWH/KMSWH/KHSWH, *Kabuli* low-/medium-/high-SW haplotype.

transcriptional regulation and expression during later stages of seed development in corresponding haplotype-introgressed NILs. These traits might collectively affect the development and growth of seeds

(cotyledons), leading to a significant decrease in SW in low- relative to high-SW NILs (Fig. 8, A and C). These consequences can be expected considering the involvement of ABC transporter genes in transportation

of GS-conjugates and dependency of seed maturation on GHS biosynthesis in the vacuoles of embryo/cotyledons of Arabidopsis seeds (Lu et al., 1998; Tommasini et al., 1998; Cairns et al., 2006).

The high- (HAP C) and low- (HAP A) SW haplotype-dependent transport assay was performed in vacuolar membrane-enriched vesicles to measure the concentration-dependent uptake of GS-conjugates such as s-2,4-dinitrophenyl glutathione (^{3}H-DNP-GS) and glutathione disulfide (^{3}H-GSSG) in the yeast cell. This demonstrated a significant difference in substrate preference and maximal transport ability between the heterologously expressed high-SW haplotype HAP C and the low-SW haplotype HAP A. The Michaelis-Menten kinetics-derived V_{max} value estimated for high-SW haplotype HAP C-dependent uptake of ^{3}H-DNP-GS and ^{3}H-GSSG was approximately twofold greater than that of low-SW haplotype HAP A (Fig. 10D). However, no such transportation ability of ^{3}H-DNP-GS and ^{3}H-GSSG was observed in the yeast heterologously expressing the low-SW haplotype.

The effects of CaABCC3(6) gene haplotypes on seed yield and quality components were compared between low- and high-SW desi and kabuli NILs, along with the mapping parental accessions and six high-yield Indian desi (ICCV 10, ICCV 93954, and ICCV 92944) and kabuli (ICCV 96329, ICC 12968, and ICCV 92311) chickpea varieties using multienvironment field phenotyping data (Fig. 11A). Compared with others, high-SW haplotype (HAP C)-introgressed desi and kabuli NILs had multiple desirable seed yield and quality attributes, including semierect plant growth habit; desirable seed color; early flowering/maturity; semidwarf plant height; and increased branch number, PN/SN, SW, yield per plant, and yield per hectare (productivity), as well as enhanced protein, GSH, thiolic amino acid (Met and Cys), iron and zinc contents, and reduced phytic acid in their seeds (Fig. 11A; Supplemental Tables S20 and S21). This implies the greater efficacy of natural alleles and the superiority of the high-SW haplotype delineated from a CaABCC3(6) gene employing an integrated genome-wide genomics strategy in developing high-yielding chickpea cultivars with enhanced seed-quality/nutritional traits. The desi NIL (DHSW[ICC 14649-NIL]$^{CaABCC3[6]DHSWH}$) harboring the CaABCC3(6) gene/haplotype (high SW) in the background of ICCV 93954 with SW 35.6 g and significant yield advantage over the parent ICCV 93954 was entered into the All India Coordinated Research Project on Chickpea trials for possible variety release after multilocation testing (Fig. 12).

DISCUSSION

Natural Alleles and Superior Haplotypes Delineated from an ABCC3(6) Gene Modulating SW in Chickpea

Large-scale discovery and high-throughput genotyping of genome-wide SNPs in a phenotypically well-characterized association panel (germplasm accessions) and in mapping populations is essential to uncover the functionally relevant genes and alleles regulating vital agronomic traits in crop plants, including chickpea. This study constituted an association panel (291 desi and kabuli germplasm accessions) and RIL mapping populations of desi and kabuli chickpea, exhibiting wide phenotypic variation as well as high heritability of three major pod and seed yield traits, including 100-SW, across multiple field environments. The high-throughput sequencing-based genotyping of these field-phenotyped natural and mapping populations using a high-resolution GBS assay detected 83,176 genome-wide SNPs, which were further employed in an integrated molecular genetics and genomics-assisted breeding approach for rapid genetic dissection of SW trait in chickpea. This genome-wide integrated strategy combining high-resolution GWAS and gene-by-gene regional association analysis with fine-mapping, map-based cloning, transcript profiling, and molecular haplotyping identified natural alleles and superior haplotypes of a CaABCC3(6) gene regulating SW variation through a zygotic effect in desi and kabuli chickpea (Supplemental Fig. S15). Therefore, an integrated genomics strategy deployed in this investigation appears much proficient for rapid delineation of promising molecular signatures governing SW in chickpea as compared to previous studies (Kujur et al., 2013, 2015a; Saxena et al., 2014a; Bajaj et al., 2015a; Das et al., 2015a, 2015b; Verma et al., 2015; Singh et al., 2016). This higher efficiency can be ascribed to combined use of a large-scale phenotypically well-characterized association panel as well as mapping populations of desi and kabuli chickpea, providing higher mapping power and resolution at a genome-wide scale.

Seed size/SW is considered a key determinant of evolutionary fitness and usually experiences tremendous changes during crop domestication. The genes associated significantly with this major domestication trait are targeted during traditional breeding and genomics-assisted crop improvement of multiple crop plants, such as rice, tomato, and chickpea (Orsi and Tanksley, 2009; Huang et al., 2013; Kujur et al., 2013, 2015a, 2016; Saxena et al., 2014a). To decipher the impact of the CaABCC3(6) gene in domestication of seed size/SW traits in chickpea, haplotypes constituted from a strong SW-associated ABCC3(6) gene were compared among 291 cultivated (desi and kabuli) and 81 wild accessions. The low- and medium-SW-associated haplotypes represented a major proportion of desi and wild accessions, while the high-SW haplotype was predominant in kabuli accessions and, interestingly, was missing from wild accessions. This reflects a major impact of strong artificial selection and evolutionary bottlenecks during domestication of these gene haplotypes and natural alleles from wild gene pools toward the assortment of the more desirable large seed size and high SW traits in cultivated chickpea. Modern breeding efforts, including inter/intraspecific hybridization
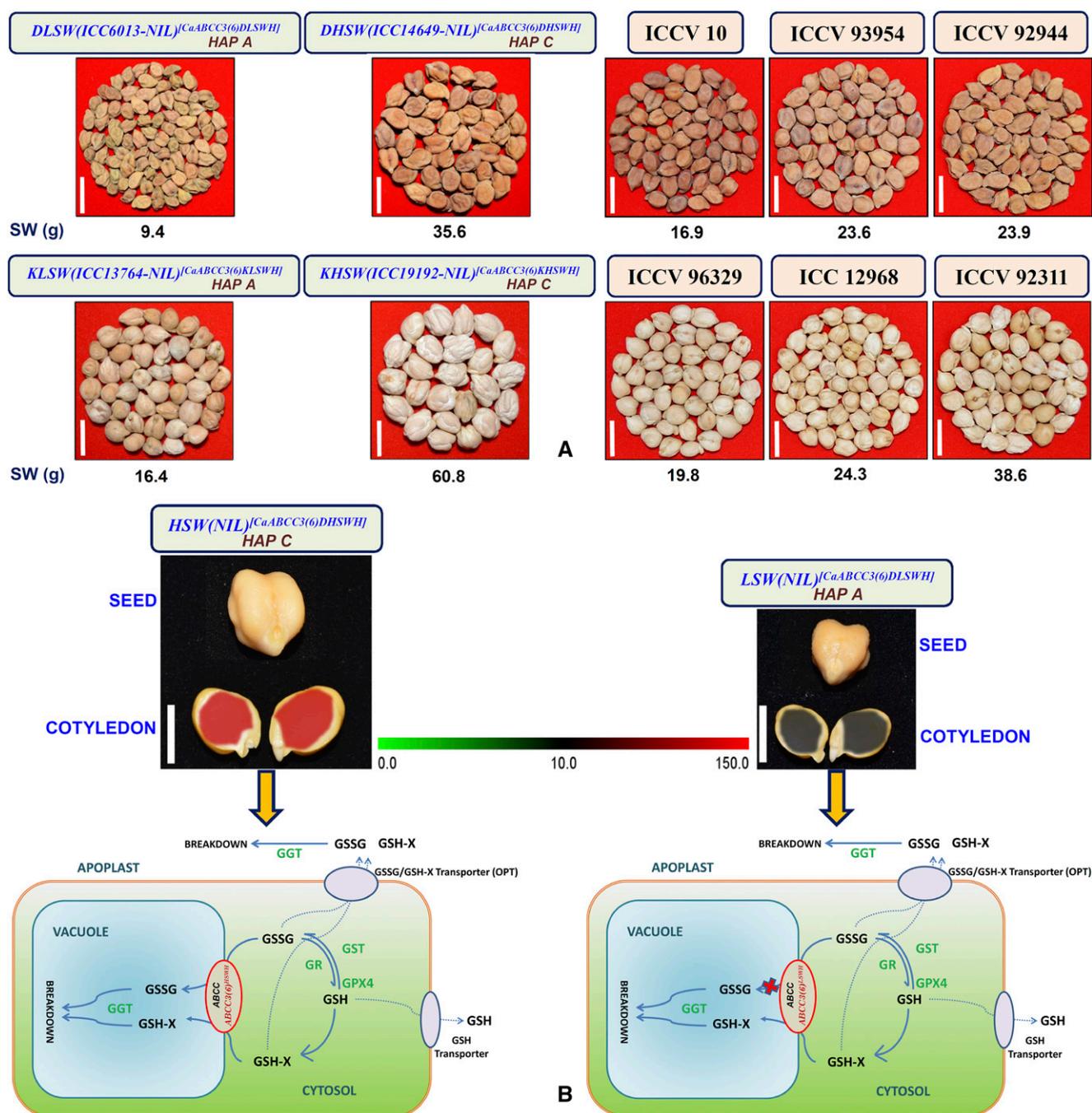
Figure 11. Modulation of GHS conjugates transportation by the superior haplotype of an ABCC3 transporter, *CaABCC3(6)*, enhances SW/yield and seed quality in the corresponding gene haplotype-introgressed NILs of *desi* and *kabuli* as compared to high-yielding Indian chickpea cultivars. A, Picture illustrating the comparative overview of seed size/SW variation observed between low- and high-SW NILs as well as high-yielding Indian varieties of *desi* and *kabuli* chickpea. The details of agronomic characteristics of these NILs and Indian varieties are mentioned in Supplemental Table S18. B, Diagrammatic representation of a plant cell playing the role of the *ABCC* transporter. The high SW (100-SW haplotype [HAP C, *ABCC3(6)^HSWH*] exhibited a greater fold of transcript expression in the seed cotyledons compared to its low SW counterpart [HAP A, *ABCC3(6)^LSWH*]). At the cellular level, the *ABCC3* transporter is localized in the vacuolar membrane where it is involved in the transportation of GSSG, and glutathione-conjugates (GS-X) from the cytosol to the vacuole. GSSG and other GS-Xs are derived from cytosolic redox conversion of GHS by several enzymes like glutathione reductase (GR), glutathione-s-transferase tau 24 (GST), and glutathione peroxidase 4 (GPX4). These GHS conjugates once inside the vacuole are degraded to their component amino acids by gamma-glutamyl transpeptidase (GGT), which may then be utilized by the cell for its growth and development. The GSSG and GS-X are transported out of the cell by oligopeptide transporters (OPTs), and the same process of breakdown of these conjugates by GGT

continuously practiced during genetic improvement of chickpea, have played a major role in enhancing diverse seed size/SW trait characteristics. The large seed size (high SW), due to its greater consumer preference and economic importance in trade and commerce, has been selected during breeding. Deciphering the natural allelic and haplotype constitution/variation of the *CaABBC3(6)* gene helped us to understand the SW trait evolution in chickpea and thus indicated a crucial role of seed size/SW in the domestication of cultivated and wild chickpea. This is consistent with earlier observations on seed size/SW evolution and trait domestication in tomato, which is governed primarily by natural allelic variants of an ABCC5-type ABC transporter gene (Orsi and Tanksley, 2009). The clues obtained here helped us to rapidly select the most favorable SW-associated potential alleles/haplotypes from a *CaABCC3(6)* gene that were naturally adapted and domesticated within the cultivated *Cicer* genepool for further genetic enhancement studies to develop *desi* and *kabuli* cultivars with high SW and yield.

ABCC3(6) Haplotype-Introgressed NILs Show Functional Significance of Superior Molecular Signatures for Enhancing SW and Other Desirable Yield and Nutritional Traits in Chickpea, Paving Way for Future Crop Improvement Endeavors

Development of NILs with high recurrent parental genome recovery minimizes the undesirable pleiotropic effects from donor parental accession in those lines. In this investigation, this was achieved by gene haplotype-assisted foreground and background selection, which led to 99.1% to 99.6% recovery of the recurrent parental genome in *CaABCC3(6)* gene haplotype-introgressed low- and high-SW NILs of both *desi* and *kabuli* chickpea. Thus, gene haplotype-assisted foreground and background selection compared with the marker-assisted selection is a superior strategy for selection of the most promising recombinants and developing haplotype-introgressed NILs in chickpea and other crop plants.
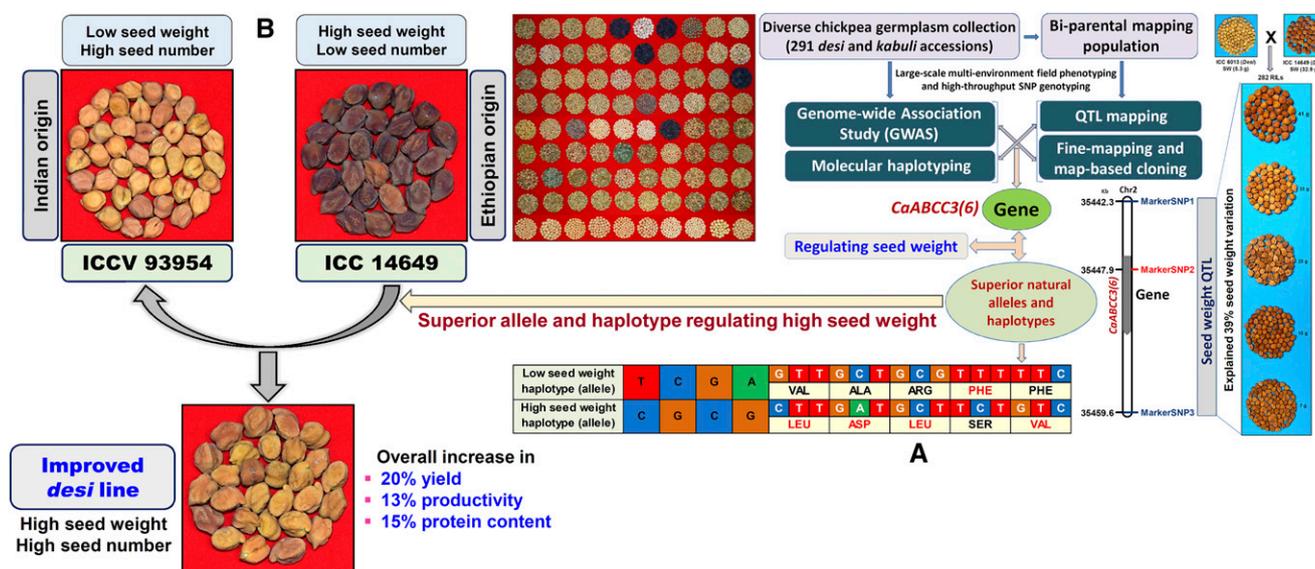
The role of the *CaABCC3(6)* gene in regulating SW differentiation was assessed through diverse functional genomics approaches, including estimation of seed GHS content and glutathione conjugate (GS) transportation assays in low- and high-SW NILs of *desi* and *kabuli* chickpea. The high-SW haplotype of the *CaABCC3(6)* gene showed greater accumulation at the transcript level compared to its low-SW counterpart

during seed development. Pronounced expression of the high-SW haplotype of the *CaABCC3(6)* gene during seed (cotyledon) maturation is in line with the enhanced transcriptional activity of its promoter from high- compared to low-SW NILs (Fig. 11B). In high-SW NILs, efficient transportation of GS-conjugates in the vacuole supplements the additional requirement of reduced sulfur (GSH) and its catabolized free thiolic amino acids (Met and Cys), especially for the synthesis of structural/metabolic as well as storage proteins during maturation of chickpea seeds (Cairns et al., 2006; Noctor et al., 2012). This is evident from the high GSH, thiolic amino acid (Met and Cys), and protein contents in mature seeds and cotyledons of high-SW NILs compared to low-SW NILs. Differential expression of *CaABCC3(6)* gene haplotypes in the cell (cytosol and vacuole) of both high- and low-SW NILs compared to the known genes involved in transportation and metabolism of GS-conjugates suggests a primary role of this gene haplotypes (alleles) in modulating the major SW variation by alteration of GS-conjugate transportation in chickpea (Fig. 11B).

The Arabidopsis gene homologs of the ABCC (such as *ABCC5* and *ABCC13*) class of transporters enhance seed size/SW as well as seed phytic acid content. These ABC transporters modulate myo-inositol-1,2,3,4,5,6-hexakisphosphate metabolism and the compartmentalization and transport of phytate in the seeds of many crop plants (Shi et al., 2007; Panzeri et al., 2011; Bhati et al., 2016). Considering the nutritional value and benefit of reduced seed phytic acid for human health, multiple efforts have been devoted to seed (embryo)-specific silencing of the *ABCC5* and *ABCC13* genes through developing genetically modified crop plants and identification of low-phytic–acid mutants in maize, wheat, and soybean (Shi et al., 2007; Bhati et al., 2014, 2016). However, very limited success has been achieved to date in this regard without compromising the agronomic performance and yield advantage of crop plants. Moreover, no such information on development of high-yielding cultivars with increased SW and low seed phytic acid content by manipulating any ABC transporter gene is documented in any crop. The high-SW NILs introgressed with a superior high-SW *CaABCC3(6)* haplotype compared to existing high-yielding *desi* and *kabuli* Indian varieties showed not only enhanced SW and yield but also improvement in multiple desirable yield and quality components, such as overall plant architecture, flowering/maturity time, plant height, branch number, PN/SW, seed color, seed protein, seed iron, seed zinc, and seed phytic acid contents.

Figure 11. (*Continued.*)
also takes place in the apoplast. The high-SW haplotype (HAP C, *ABCC3*[6]^{HSWH}) as compared to low SW haplotype (HAP A, *ABCC3*[6]^{LSWH}) is more efficient in the vacuolar transport of GSSG and GHS-conjugate like DNP-GS as well as their subsequent metabolism in the cell through transcriptional regulation by inducing transcript expression and accumulation in the vacuoles of seeds and cotyledons at the mature stage. This overall enhances the growth, development, and maturation of seeds and cotyledons in high- vis-à-vis low-SW haplotype-introgressed NILs and thereby increases the thiolic amino acid (Met and Cys) and protein contents in seeds of *desi* and *kabuli* chickpea. Scale bar = 1 cm. DLSW/KLSW, *Desi/kabuli* low SW; DHSW/KHSW, *Desi/kabuli* high SW; LSWH/HSWH, low-/high-SW haplotype.

Mining, Genotyping, and Annotation of Genome-Wide SNPs

The 96-plex GBS libraries constructed from the genomic DNA of all 291 germplasm accessions (association panel) and 384 mapping individuals and parental accessions of two RIL populations were sequenced using an Illumina HiSeq2000 (Illumina) Next-Generation Sequencing platform. The demultiplexed high-quality sequences after quality filtering were mapped to the reference *kabuli* genome (Varshney et al., 2013, http://gigadb.org/dataset/100076). The high-quality SNPs mined from the diverse coding and noncoding sequence components of *kabuli* genes (Varshney et al., 2013; http://gigadb.org/dataset/100076) and genomes (chromosomes/pseudomolecules and unanchored scaffolds) were structurally and functionally annotated. To accomplish this, detailed procedures following Kujur et al. (2015a, 2015b, 2015c are illustrated in Supplemental Figure S2. Briefly, we used customized Perl scripts and a single-nucleotide polymorphism effect predictor (SnpEff v3.1h; http://snpeff.sourceforge.net) to infer the accurate genomic distribution including the structural and functional annotation of the mined SNPs. The SNPs with synonymous and nonsynonymous substitutions were plotted in accordance with their unique physical positions (bp) on the eight chromosomes (pseudomolecules) of the *kabuli* genome and were visualized by Circos (Krzywinski et al., 2009). The putative functions of genes with SNPs were determined based on the *kabuli* genome annotation (Varshney et al., 2013; http://gigadb.org/dataset/100076) and PFAM database v27.0 (http://pfam.sanger.ac.uk) as per Kujur et al. (2015b) and Srivastava et al. (2016).

Estimation of Molecular Diversity, Population Genetic Structure, and LD Pattern

The genome-wide GBS-derived SNP genotyping information was analyzed with PowerMarker v3.51 (Liu and Muse, 2005) and the 100-kb nonoverlapping sliding window approach of TASSEL v5.0 (Bradbury et al., 2007; http://www.maizegenetics.net) to measure the polymorphism information content and nucleotide diversity parameters ($\theta\pi$, $\theta\omega$, and Tajima's D), respectively, among all 291 *desi* and *kabuli* chickpea accessions belonging to an association panel following Kujur et al. (2015b).

The genome-wide SNP genotyping data were put into PowerMarker, STRUCTURE v2.3.4 (Pritchard et al., 2000). and MEGA7 (Tamura et al., 2007), to determine the molecular diversity and population genetic structure and for constructing the unrooted neighbor-joining phylogenetic tree (Nei et al., 1983; Nei's genetic distance with 1,000 bootstrap replicates) among the 291 *desi* and *kabuli* chickpea accessions following the methods described by Kujur et al. (2015a, 2015b). In the population structure, the optimal population number (K) was determined using the "ad hoc" and "delta K" procedures of Pritchard et al. (2000) and Evanno et al. (2005), respectively.

The genome-wide LD pattern (r^2, frequency correlation between pairs of alleles across pairs of SNP loci), including LD decay (by plotting average r^2 against a 50-kb uniform physical interval across the eight chromosomes), were determined in the *desi* and *kabuli* accessions as well as in the population (defined by population genetic structure) of a constituted association panel of chickpea. For this, the genotyping data of SNPs physically mapped on chromosomes were analyzed using a command (--r2--ld-window 99999--ld-window-r2 0) in PLINK (Purcell et al., 2007) and the full-matrix approach of TASSEL (following Zhao et al., 2011; Kujur et al., 2015b). The ANOVA-based significance test of LD estimates was performed by comparing the r^2 values across accessions/population and chromosomes using the software SPSS v17.0 (http://www.spss.com/statsistics) as per Saxena et al. (2014b).

GWAS

For trait association mapping, the genome-wide SNP genotyping data were integrated with multienvironment (three years) replicated field phenotyping data of three major seed and pod yield traits (PN, SN, and SW) as well as population structure, kinship, and PCA information of the 291 *desi* and *kabuli* accessions belonging to an association panel of chickpea. The PCA and K matrix among accessions was estimated by GAPIT (Lipka et al., 2012) and SPAGeDi 1.2 (Hardy and Vekemans, 2002), respectively. These were further analyzed with the CMLM (Zhang et al., 2010) interfaces of GAPIT as per Kujur et al. (2015a) and Kumar et al. (2015). To improve the accuracy of SNP marker-trait association in the GWAS, the quantile–quantile plot-based Benjamini and Hochberg false discovery rate (FDR; cutoff $\leq$ 0.05) corrections for multiple comparisons

between observed/expected $-\log_{10}(P)$ values and the adjusted *P*-value threshold of significance were performed. Based on these, the SNP loci significantly associated with PN, SN, and SW were identified by individual year-wise and among the three years overall at a lowest *FDR*-adjusted *P* value (threshold *P*) of $< 1 \times 10^{-4}$ and the highest R^2 in the *desi* and *kabuli* accessions, as well as in the population (defined by population genetic structure) of chickpea. The magnitude (R^2) of PVE for the studied yield traits by the *FDR*-controlling method of the model with the SNP (adjusted *P* value) was estimated.

Genetic Linkage Map Construction and High-Resolution QTL Mapping

The genotyping data of genome-wide GBS-SNPs (exhibiting polymorphism between parental accessions) obtained from 282 and 190 mapping individuals of two intraspecific RIL populations (ICC 6013 × ICC 14649 and ICC 13764 × ICC 19192, respectively) were used to construct the genetic linkage maps at the LOD threshold (4.0–10.0) with the Kosambi mapping function following Kujur et al. (2015c) and Srivastava et al. (2016). A consensus genetic linkage map derived from two intraspecific genetic maps was constructed using JoinMap 4.1 [as per Bohra et al. (2012) and Varshney et al. (2014)] in accordance with the centiMorgan genetic distances and respective marker physical positions (bp) on eight linkage groups (LGs; designated LG1–LG8)/chromosomes and further visualized using the software package Circos following Das et al. (2015b).

For high-resolution QTL mapping, the genotyping data of parental polymorphic GBS-SNPs genetically mapped on two intraspecific and a consensus genetic linkage map (comprising eight LGs/chromosomes) was correlated with multienvironment (years) field phenotypic data of three major pod- and seed-yield traits (PN, SN, and SW) of two RIL mapping populations using a composite interval mapping function (LOD > 4.0 with 1,000 permutations and P $\leq$ 0.05) within MapQTL 6 (van Ooijen, 2009) as per Das et al. (2015b) and Kujur et al. (2015c). The PVE (%) as well as positional and additive effect (evaluated by parental origin of favorable alleles) specified by each significant PN, SN, and SW QTL were measured at a significant LOD (P $\leq$ 0.05) as per Bajaj et al. (2015b). The additive effect of SNPs harboring the QTLs and pleiotropic QTLs were determined using QTL Network v2.0 and multiple-trait composite interval mapping of QTL Cartographer, respectively. The confidence interval of each significant major QTL peak was evaluated by using ±1-LOD support intervals (95% confidence interval).

Regional Association Analysis and Molecular Haplotyping

The 250-kb genomic regions flanking the 12-GWAS–derived PN, SN, and SW trait-associated genes and a 437.7-kb genomic interval underlying a major SW QTL (*CaqSW2.4*; identified by high-resolution QTL mapping) were targeted for regional association analysis, and a strongly SW-associated ABC transporter gene was selected for molecular haplotyping. The selected genomic/gene regions were sequenced using the genomic DNA of the 291 *desi* and *kabuli* accessions (association panel) and 81 wild *Cicer* accessions employing the multiplexed amplicon-sequencing protocol (following the manufacturer's instructions) of TruSeq Custom Amplicon v1.5 in the Illumina MiSeq Next-Generation Sequencing platform. The custom oligo probes targeting the selected genomic regions, including CDSs/exons, introns, 2-kb upstream regulatory regions (URRs), and 2-kb downstream regulatory regions of genes, were designed and synthesized using Illumina Design Studio. The probes producing amplicons with an average size of 500 bp per reaction were pooled into the custom amplicon tubes, and the template libraries were constituted. The sample-specific indices were added to each library by PCR using common primers, and the uniquely tagged pooled amplicon libraries were normalized. The generated clusters were sequenced by the Illumina MiSeq platform. Visualization/mapping of sequenced amplicons and discovery of high-quality sequence variants (SNPs) among accessions were performed as per Saxena et al. (2014b), Kujur et al. (2015c), and Malik et al. (2016). The mapping of high-quality amplicon sequence reads onto the reference *kabuli* chickpea genome and the detection of SNPs and their structural and functional annotation were performed by adopting the aforesaid methods, as described in Supplemental Figure S2. The constitution of SNP haplotypes in the genes and sequenced genomic regions and determination of SNP haplotype-based LD and domestication patterns, as well as estimation of the association potential of the haplotypes with the studied yield traits, were done following Saxena et al. (2014b) and Kujur et al. (2015a).

Fine-Mapping and Map-Based Cloning

To fine-map a major SW QTL (*CaqSW2.4*) identified by high-resolution QTL mapping, four low- or high-SW NILs (BC$_4$F$_3$) of *desi* and *kabuli* chickpea were developed by introgressing the shorter (76-kb) genomic intervals of target SW QTLs following the strategies depicted in Figure 5. The generated low- and high-SW NILs from each *desi* and *kabuli* were intercrossed separately (cultivar-wise) to develop two *desi* and *kabuli* F2 mapping populations consisting of 380 and 277 individuals, respectively. For high-resolution molecular mapping of a SW QTL (*CaqSW2.4*), these mapping individuals were genotyped by amplicon-resequencing–based SNPs using the Sequenom Matrix-Assisted Laser Desorption Ionization Time-of-Flight MassARRAY assay as per http://www.sequenom.com and Saxena et al. (2014a, 2014b). Subsequently, the NIL mapping individuals were phenotyped for SW in the field, and QTL mapping was performed as per the aforesaid strategy.

For marker (haplotype)-assisted foreground selection, the SNPs flanking/tightly linked to a *CaqSW2.4* major QTL, as well as a strongly SW-associated ABC transporter gene and its low- and high-SW gene haplotypes, were genotyped among mapping individuals of the back-cross–mapping population using a MALDI-TOF assay following Saxena et al. (2014a, 2014b; Fig. 5). Likewise, for marker (haplotype)-assisted background selection, 1,536 SNPs mapped uniformly across the eight chromosomes of the *kabuli* genome were genotyped in the selected back-crossed lines using a Matrix-Assisted Laser Desorption Ionization Time-of-Flight assay (Fig. 5). For large-scale phenotyping of back-cross–mapping populations, the individuals were phenotyped in the field in a randomized complete block design (RCBD) with at least three replications. The SW was measured by estimating the average weight (g) of 100 matured seeds at 10% moisture content from 20 to 30 representative plants (selected from the middle of each row) of each progeny as per Kujur et al. (2015a, 2015b).

For the progeny analysis, the homozygous recombinant and homozygous nonrecombinant individuals derived from the low- and high-SW NILs of *desi* and *kabuli* chickpea were selected based on their genetic constitution and the recombination among SNPs flanking/tightly linked to a major SW QTL (*CaqSW2.4*) as well as a strongly SW-associated ABC transporter gene and its low- and high-SW gene haplotypes. The selected recombinant and nonrecombinant progenies were grown in the field as per RCBD with three replications, and individual progenies were phenotyped precisely for SW following the aforesaid methods. The significant variation of SW between selected recombinant and nonrecombinant progenies was evaluated by a one-tailed Student's *t* test. To phenotype the developed low- and high-SW ABC transporter gene haplotype-introgressed NILs for diverse agronomic traits, these lines along with four RIL mapping parental accessions (ICC 6013, ICC 14649, ICC 13764, and ICC 19192) and a total of six high-yielding *desi* (ICCV 10, ICCV 93954, and ICCV 92944) and *kabuli* Indian varieties (ICCV 96329, ICC 12968, and ICCV 92311) were grown in the field as per RCBD with three replications.

Differential Expression Profiling

To detect differential gene regulatory function, the expression profiling of strongly SW-associated genes was performed using semiquantitative and quantitative RT-PCR assays. RNA was isolated from vegetative (root, shoot, and leaf) and reproductive tissues (flower, pod, cotyledon, and mature seed) and seed development stages (DS1 [0–10 DAP], DS2 [11–20 DAP], DS3 [21–30 DAP], and DS4 [31–40 DAP]) of RIL mapping parental accessions (ICC 6013, ICC 14649, ICC 13764, and ICC 19192) and the 76-kb major SW QTL (*CaqSW2.4*)-introgressed NILs of *desi* and *kabuli* chickpea with contrasting low and high SW. The expression analysis was performed by assaying the gene-specific primers in tissues of accessions/NILs as per Bajaj et al. (2015a) and Upadhyaya et al. (2015). Briefly, 1 μg of high-quality RNA isolated from the tissues/stages was used to synthesize cDNA with an Applied Biosystems cDNA synthesis kit. The diluted cDNA and 1X Fast SYBR Green Master Mix (Applied Biosystems) and 200 nM of forward and reverse gene-based primers were amplified in an ABI7500 Fast RT-PCR system. Biological and technical replicates along with an internal control gene, *elongation factor 1-alpha*, were utilized for expression profiling in the RT-PCR assay as recommended by Bajaj et al. (2015a). Significant differences in gene expression were estimated, and expression profiles were visualized with a heat map by MultiExperiment Viewer (http://www.tm4.org/mev). Similarly, RNA isolated from the aforementioned vegetative and reproductive tissues as well as four seed development stages (DS1–DS4) of low- and high-SW gene haplotype-introgressed NILs were amplified with the corresponding low- and high-SW gene haplotype-specific primers following the methods of the expression assay described

above. We followed a similar experimental strategy for differential expression profiling to infer the regulatory functions of Arabidopsis homologs of chickpea genes known to govern transport and metabolism of GHS in the cell (cytosol and vacuole).

Northern Hybridization

For Northern assays, high-quality RNA (10–20 μg) isolated from the seeds (DS4) and cotyledons of low- and high-SW gene haplotype-introgressed NILs was transferred into a Nylon membrane to prepare the RNA blots in accordance with Doblin et al. (2001). To make the radiolabeled probe, RNA isolated from low- and high-SW ABC transporter gene haplotype-introgressed NILs was amplified using the corresponding low- and high-SW haplotype-specific primers targeting the complete CDS of a strong SW-associated gene (producing a 4.2-kb amplicon), and the amplicon was further labeled with α-P^{32}-dCTP using a random-primer labeling kit (MBI; Fermentas). The RNA blots were hybridized with denatured radiolabeled probe, washed, exposed to a phosphorimaging K-Screen (Bio-Rad) and visualized using a PharosFX phosphoimager following Kujur et al. (2015a).

Transient Expression Assay

The upstream regulatory (promoter) region of low-, medium-, and high-SW haplotypes constituted from a strongly SW-associated ABC transporter gene were amplified from DNA of low- and high-SW haplotype-introgressed NILs as well as *desi* (ICC 8318 [SW: 18.2 g] and ICC 14626 [18.3 g]) and *kabuli* chickpea accessions (ICC 7272 [28.2 g] and ICC 7654 [29.1 g]) exhibiting medium SW variation. The amplified promoter region was further cloned into a binary plasmid vector pCAMBIA1301 to drive expression of *GUS* reporter protein. Subsequently, *Agrobacterium tumefaciens* strain EHA105 consisting of this recombinant plasmid along with another plasmid vector, pCAMBIA1302, expressing GFP (*GFP*; used for normalization of transformation efficiency), were agro-infiltrated into young leaves of two-month-old chickpea accession ICCV 93954 following Dwivedi et al. (2017). Quantitative RT-PCR was used to measure the normalization of transformation efficiency by estimating the fold-change in GFP transcript expression. Accordingly, GUS activity was measured by inferring the normalized transcript abundance of the *GUS* gene from three haplotype constructs as per Dwivedi et al. (2017). Six biological replicates, each with at least three technical replicates, giving a total of 108 measurements of each haplotype construct, were assayed for the transient expression study.

Annotation and Genomic Constitution of ABC Transporters

A genome-wide scan was performed to identify the diverse class of genes coding for ABC transporter annotated from the *kabuli* chickpea genome (Varshney et al., 2013; http://gigadb.org/dataset/100076) through a HMMER search taking an e-value cutoff of 1e-05 (http://hmmer.org). The hidden Markov model profile was built based on the available ABC transporter protein sequence resources from the National Center for Biotechnology Information (NCBI; https://www.ncbi.nlm.nih.gov). The resultant sequences were further analyzed in INTERPRO (https://www.ebi.ac.uk/interpro) to infer their signature nucleotide-binding folds. The ABC transporters were further categorized based on the types of domains in the amino acid sequences encoded by these genes and their homology with their Arabidopsis counterpart. The distribution of the identified ABC transporter genes was determined in accordance with their physical positions on the eight chromosome pseudomolecules of the *kabuli* genome and was visualized by a MapChart (Voorrips, 2002).

Yeast Complementation Assay

Wild-type parent yeast strain YPH299 and Δ*ycf1*, a known vacuolar GHS s-conjugate transporter mutant, were used for the complementation assay of low- and high-SW ABC transporter gene haplotypes. Two different constructs, comprising low- and high-SW ABC transporter gene haplotypes cloned in pYES260, were used to transform the Δ*ycf1* mutant strain for the complementation assay following the experimental strategies described by Bhati et al. (2014, 2015).

Subcellular Localization

The amino acid sequences encoded by the full-length CDS of SW-associated ABC transporter gene haplotypes were analyzed using WoLF PSORT for in silico prediction of a localization signal sequence (https://www.genscript.com/wolf-psort.html). For experimental validation of its subcellular localization, the ~500-bp amplicons targeting the predicted localization signal sequences at the nonsynonymous SNP-containing transmembrane domain of each low- and high-SW-associated gene haplotype were amplified from the low- and high-SW haplotype-introgressed NILs using the corresponding haplotype-specific primers. These low- and high-SW ABC transporter gene haplotype-specific amplicons were further cloned into the Gateway Entry vector pENTRTM/D-TOPO (Invitrogen) using Gateway technology according to the manufacturer's instructions. An LR (LR Clonase II, Invitrogen) reaction was used to transfer the resulting low- and high-SW gene haplotype constructs into the destination N-terminal yellow fluorescent protein (YFP) fusion vector (pSITE-YFP3CA) to generate the gene haplotype-YFP fusion constructs, under the control of a duplicated cauliflower mosaic virus (CaMV) 35S promoter. The accuracy of constructs was further confirmed by sequencing as per Kujur et al. (2013). These haplotype constructs were transiently expressed in normal and plasmolyzed (10% w/v mannitol solution) onion epidermal cells by microprojectile particle bombardment using a Biolistic-PDS-1000/He Particle Delivery System (Bio-Rad) in accordance with the manufacturer's instructions. After 12–18-h incubation at 28°C, the onion peels were observed under a TCS-SP2 Confocal Laser Scanning Microscope (Leica) for YFP and red fluorescent protein (RFP) signals at 514 nm and 561 nm, respectively. To determine whether the in silico subcellular localization of low- and high-SW ABC transporter gene haplotypes was in the vacuole, an Arabidopsis VIT1 protein fused with RFP was used as a vacuole-specific marker.

NIL Reciprocal Cross Development and Phenotyping

The reciprocal F1 crosses were made by intercrossing the high- and low-SW ABC transporter gene haplotype-introgressed NILs between each other. The F1 reciprocal lines and selfed individuals from the developed NILs were phenotyped in the field as per RCBD with three replications, and the SW was measured as described in Kujur et al. (2015a).

Seed Development Study

The parental accessions (ICC 6013, ICC 14649, ICC 13764, and ICC 19192) of two RIL mapping populations as well as ABC transporter gene haplotype-introgressed NILs with low and high SW were grown in the field and greenhouse as per RCBD with two replications. At least 10 healthy seeds were harvested individually from 20 representative plants (selected from the middle of each row) of each accession/NIL at four seed development stages, DS1 (0–10 DAP), DS2 (11–20 DAP), DS3 (21–30 DAP), and DS4 (31–40 DAP). The weights (mg) of the entire mature seed, embryo, and endosperm obtained from diverse developmental stages of seeds were measured in 20 biological replicates, each with at least three technical replicates. The tissues representing those four developmental stages of seeds with suitable biological/technical replicates were visualized under a light microscope (Leedz Micro Imaging). The morphometric features such as area, width, and height of the entire seed, embryo, and cotyledon at different seed development stages of low- and high-SW NILs and RIL mapping parental accessions were estimated by using the software ImageJ v1.31 (http://rsb.info.nih.gov/ij/).

Estimation of Seed Protein, Seed GHS, Seed Phytic Acid, and Seed Amino Acid Contents

The mature seeds, including cotyledons from each parental accession (ICC 6013, ICC 14649, ICC 13764, and ICC 19192) of two RIL mapping populations as well as ABC transporter gene haplotype-introgressed NILs of *desi* and *kabuli* chickpea with low and high SW (biological/technical replicates), were used to estimate the protein, GHS, phytic acid, and amino acid contents. The protein content was estimated following Upadhyaya et al. (2016). GSH content was measured using a fluorometer and reverse-phase liquid chromatography as per Lu et al. (1998), Cairns et al. (2006), and Dragićević et al. (2015). The phytic acid was estimated in accordance with Gao et al. (2007) and Joshi-Saha and Reddy (2015). Amino acid content was calculated using the amino acid analyzer chromatography and UltraViolet-Visible spectrophotometric methods as

previously described in Moore et al. (1958), Ohkama-Ohtsu et al. (2007), and Okoronkwo et al. (2017).

GHS-Conjugates Transport Assay

To estimate the low- and high-SW ABC transporter gene haplotype-dependent GHS-conjugate transport in the vacuole, the vacuolar membrane and crude vacuolar membrane vesicles from seeds and cotyledons of low- and high-SW ABC transporter gene haplotype-introgressed NILs were isolated (biological/technical replicates), and the protein concentration of vacuolar membranes from these NILs was measured as described by Li et al. (2014). The preparation and purification of the GSH conjugates H-DNP-GS and ^{3}H-GSSG and the measurement of their transport by a GSH conjugate transportation assay were performed according to Lu et al. (1998).

Availability of Data and Materials

The sequencing data has been submitted in NCBI-Sequence Read Archive database (http://www.ncbi.nlm.nih.gov/sra) with Submission ID: SUB3039352 (Sequence Read Archive ID: SRR6062136). All high-quality SNPs discovered were submitted to NCBI dbSNP (http://www.ncbi.nlm.nih.gov/SNP/snp_viewTable.cgi?handle=NIPGR; Supplemental Tables S3 and S4) for unrestricted public access.

Accession Numbers

The gene sequence information can be found in GIGADB DATASETS under the following *Cicer_arietinum_GA_v1.0* accession numbers: ABC transporters, *CaABCC3(6)* and *Ca_09705*; and cation transporter, *Ca_09704*. The accession numbers of genome-wide identified ABC transporter genes can be found in Supplemental Table S17.

Supplemental Data

The following supplemental materials are available.

Supplemental Figure S1. Major strategies adopted to select 291 phenotypically and genotypically diverse chickpea accessions belonging to an association panel for GWAS of three major pod/seed yield traits in chickpea.

Supplemental Figure S2. Schematic depicting the overall major strategy followed in a *kabuli* reference genome-based GBS assay for large-scale discovery and high-throughput genotyping of 83,176 genome-wide SNPs.

Supplemental Figure S3. Structural annotation of the genome-wide SNPs.

Supplemental Figure S4. A genome scan plot depicting the gaps represented by density of SNPs physically mapped across eight chromosomes of *kabuli* genomes.

Supplemental Figure S5. Proportion of SNPs discovered from diverse TF-encoding genes representing multiple TF gene families of chickpea.

Supplemental Figure S6. Flowchart depicting an overview of CMLM-based GWAS.

Supplemental Figure S7. Circos circular ideograms depicting the genomic distribution of 12 major PN, SN, and 100-SW QTLs.

Supplemental Figure S8. Schematic illustrating the comprehensive strategies followed to develop high and low SW NILs of *desi* as well as high and low SW NILs of *kabuli* chickpea.

Supplemental Figure S9. Genomic distribution and constitution of 139 ABC transporter genes scanned and annotated from *kabuli* chickpea genome.

Supplemental Figure S10. Genome-wide distribution and constitution of ABCC-type transporters scanned and annotated from *kabuli* chickpea genome vis-à-vis Arabidopsis.

Supplemental Figure S11. Physical maps of chromosome 2, illustrating the accurate positions of 76-kb introgressed genomic *CaqSW2.4*.

Supplemental Figure S12. Phenotyping depicting the SW trait variation in self-pollinated low and high SW *desi* and *kabuli* NILs as well as in reciprocal F1 crosses.

Supplemental Figure S13. Physical estimation exhibiting variation in an average weight (mg) of single seed during development stages (DS1–DS4) of seeds including embryo and cotyledons of low and high SW *desi* and *kabuli* NILs as well as *desi* and *kabuli* mapping parental accessions.

Supplemental Figure S14. Differential expression profile of five known genes involved in metabolism and transport of GHS.

Supplemental Figure S15. Schematic illustrating a brief summary of major integrated genomics-assisted breeding.

Supplemental Table S1. Germplasm accessions included in a constituted association panel for GWAS of three major pod/seed yield traits in chickpea.

Supplemental Table S2. Summary of sequencing statistics generated by sequencing of 291 chickpea accessions (association panel) using a GBS assay.

Supplemental Table S3. Genome-wide structural and functional annotation of SNPs discovered through GBS of 291 *desi* and *kabuli* chickpea accessions (association panel).

Supplemental Table S4. SNP genotyping data (Hapmap formatted) generated by sequencing of 291 chickpea accessions (association panel) using a GBS assay.

Supplemental Table S5. Distribution of SNPs per 100-kb physical region across the eight chromosomes of the *kabuli* chickpea genome.

Supplemental Table S6. Polymorphism and molecular diversity potential of 83,176 genome-wide SNPs estimated in 291 chickpea accessions (association panel) using diverse statistical measures.

Supplemental Table S7. Descriptive statistics of three major pod/seed yield traits measured in an association panel consisting of 291 *desi* and *kabuli* chickpea accessions based on their multienvironment-replicated phenotyping in field.

Supplemental Table S8. ANOVA-based summary effects of three major pod/seed yield traits across three experimental years in 291 *desi* and *kabuli* chickpea accessions (association panel).

Supplemental Table S9. Chromosome-wise LD estimates in 291 *desi* and *kabuli* chickpea accessions (association panel) using 64,172 SNPs.

Supplemental Table S10. LD estimates among linked and global SNP-pairs in two model-based individual populations and the entire population.

Supplemental Table S11. Genomic SNP loci significantly associated with three major pod/seed yield traits in chickpea.

Supplemental Table S12. SNPs discovered from 12 SW-associated genes for gene-by-gene regional association analysis in chickpea.

Supplemental Table S13. SNPs mapped on eight chromosomes of two intraspecific genetic linkage maps ([ICC 6013 × ICC 14649] and [ICC 13764 × ICC 19192]) and a consensus genetic linkage map of chickpea.

Supplemental Table S14. Statistical measures estimated for three major pod/seed yield traits in parental accessions and 282 mapping individuals of a *desi* RIL population (ICC 6013 × ICC 14649).

Supplemental Table S15. Statistical measures estimated for three major pod/seed yield traits in parental accessions and 190 mapping individuals of a *kabuli* RIL population (ICC 13764 × ICC 19192).

Supplemental Table S16. Molecular mapping of three major pod/seed yield traits in chickpea.

Supplemental Table S17. Genome-wide distribution and constitution of ABC transporter genes in chickpea.

Supplemental Table S18. Wild *Cicer* accessions utilized for molecular haplotyping.

Supplemental Table S19. Chickpea orthologs of known Arabidopsis genes involved in transportation and metabolism of GSH in a cell including vacuole and cytosol.

Supplemental Table S20. Seed yield and quality component traits evaluated in developed low- and high-SW NILs of *desi* and *kabuli* vis-à-vis recurrent and donor mapping parental accessions and high-yielding Indian varieties of chickpea.

Supplemental Table S21. Comparative assessment of desirable agronomic trait characteristics between low- and high-SW (SW) NILs of *desi* and *kabuli* chickpea.

LITERATURE CITED

Abbo S, Molina C, Jungmann R, Grusak MA, Berkovitch Z, Reifen R, Kahl G, Winter P, Reifen R (2005) Quantitative trait loci governing carotenoid concentration and weight in seeds of chickpea (*Cicer arietinum* L.). Theor Appl Genet **111:** 185–195

Agarwal P, Kapoor S, Tyagi AK (2011) Transcription factors regulating the progression of monocot and dicot seed development. BioEssays **33:** 189–202

Bajaj D, Saxena MS, Kujur A, Das S, Badoni S, Tripathi S, Upadhyaya HD, Gowda CLL, Sharma S, Singh S, et al (2015a) Genome-wide conserved non-coding microsatellite (CNMS) marker-based integrative genetical genomics for quantitative dissection of seed weight in chickpea. J Exp Bot **66:** 1271–1290

Bajaj D, Upadhyaya HD, Khan Y, Das S, Badoni S, Shree T, Kumar V, Tripathi S, Gowda CLL, Singh S, et al (2015b) A combinatorial approach of comprehensive QTL-based comparative genome mapping and transcript profiling identified a seed weight-regulating candidate gene in chickpea. Sci Rep **5:** 9264

Berger JD, Buck R, Henzell JM, Turner NC (2005) Evolution in the genus *Cicer* vernalisation response and low temperature pod set in chickpea (*C. arietinum* L.) and its annual wild relatives. Aust J Agric Res **56:** 1191–1200

Bhati KK, Aggarwal S, Sharma S, Mantri S, Singh SP, Bhalla S, Kaur J, Tiwari S, Roy JK, Tuli R, et al (2014) Differential expression of structural genes for the late phase of phytic acid biosynthesis in developing seeds of wheat (*Triticum aestivum* L.). Plant Sci **224:** 74–85

Bhati KK, Sharma S, Aggarwal S, Kaur M, Shukla V, Kaur J, Mantri S, Pandey AK (2015) Genome-wide identification and expression characterization of ABCC-MRP transporters in hexaploid wheat. Front Plant Sci **6:** 488

Bhati KK, Alok A, Kumar A, Kaur J, Tiwari S, Pandey AK (2016) Silencing of *ABCC13* transporter in wheat reveals its involvement in grain development, phytic acid accumulation and lateral root formation. J Exp Bot **67:** 4379–4389

Bohra A, Saxena RK, Gnanesh BN, Saxena K, Byregowda M, Rathore A, Kavikishor PB, Cook DR, Varshney RK (2012) An intra-specific consensus genetic map of pigeonpea [*Cajanus cajan* (L.) *Millspaugh*] derived from six mapping populations. Theor Appl Genet **125:** 1325–1338

Bradbury PJ, Zhang Z, Kroon DE, Casstevens TM, Ramdoss Y, Buckler ES (2007) TASSEL: Software for association mapping of complex traits in diverse samples. Bioinformatics **23:** 2633–2635

Branca A, Paape TD, Zhou P, Briskine R, Farmer AD, Mudge J, Bharti AK, Woodward JE, May GD, Gentzbittel L, et al (2011) Whole-genome nucleotide diversity, recombination, and linkage disequilibrium in the model legume *Medicago truncatula*. Proc Natl Acad Sci USA **108:** E864–E870

Cairns NG, Pasternak M, Wachter A, Cobbett CS, Meyer AJ (2006) Maturation of Arabidopsis seeds is dependent on glutathione biosynthesis within the embryo. Plant Physiol **141:** 446–455

Das S, Upadhyaya HD, Bajaj D, Kujur A, Badoni S, Laxmi, Kumar V, Tripathi S, Gowda CL, Sharma S, et al (2015a) Deploying QTL-seq for rapid delineation of a potential candidate gene underlying major trait-associated QTL in chickpea. DNA Res **22:** 193–203

Das S, Upadhyaya HD, Srivastava R, Bajaj D, Gowda CLL, Sharma S, Singh S, Tyagi AK, Parida SK (2015b) Genome-wide insertion-deletion (InDel) marker discovery and genotyping for genomics-assisted breeding applications in chickpea. DNA Res **22:** 377–386

Doblin MS, De Melis L, Newbigin E, Bacic A, Read SM (2001) Pollen tubes of *Nicotiana alata* express two genes from different beta-glucan synthase families. Plant Physiol **125:** 2040–2052

Dragičević V, Kratovalieva S, Dumanović Z, Dimov Z, Kravić N (2015) Variations in level of oil, protein, and some antioxidants in chickpea and peanut seeds. Chem Biol Technol Agri **2:** 2

Dwivedi V, Parida SK, Chattopadhyay D (2017) A repeat length variation in *myo*-inositol monophosphatase gene contributes to seed size trait in chickpea. Sci Rep **7:** 4764

Evanno G, Regnaut S, Goudet J (2005) Detecting the number of clusters of individuals using the software STRUCTURE: A simulation study. Mol Ecol **14:** 2611–2620

Gao Y, Shang C, Maroof MAS, Biyashev RM, Grabau EA (2007) A modified colorimetric method for phytic acid analysis in soybean. Crop Sci **47:** 1797–1803

Ge L, Yu J, Wang H, Luth D, Bai G, Wang K, Chen R (2016) Increasing seed size and quality by manipulating BIG SEEDS1 in legume species. Proc Natl Acad Sci USA **113:** 12414–12419

Hardy OJ, Vekemans X (2002) SPAGeDi: A versatile computer program to analyse spatial genetic structure at the individual or population levels. Mol Ecol Notes **2:** 618–620

Huang R, Jiang L, Zheng J, Wang T, Wang H, Huang Y, Hong Z (2013) Genetic bases of rice grain shape: So many genes, so little known. Trends Plant Sci **18:** 218–226

Jain M, Misra G, Patel RK, Priya P, Jhanwar S, Khan AW, Shah N, Singh VK, Garg R, Jeena G, et al (2013) A draft genome sequence of the pulse crop chickpea (*Cicer arietinum* L.). Plant J **74:** 715–729

Joshi-Saha A, Reddy KS (2015) Repeat length variation in the 5'UTR of myo-inositol monophosphatase gene is related to phytic acid content and contributes to drought tolerance in chickpea (*Cicer arietinum* L.). J Exp Bot **66:** 5683–5690

Klein M, Burla B, Martinoia E (2006) The multidrug resistance-associated protein (MRP/ABCC) subfamily of ATP-binding cassette transporters in plants. FEBS Lett **580:** 1112–1122

Krzywinski M, Schein J, Birol I, Connors J, Gascoyne R, Horsman D, Jones SJ, Marra MA (2009) Circos: An information aesthetic for comparative genomics. Genome Res **19:** 1639–1645

Kujur A, Bajaj D, Saxena MS, Tripathi S, Upadhyaya HD, Gowda CLL, Singh S, Jain M, Tyagi AK, Parida SK (2013) Functionally relevant microsatellite markers from chickpea transcription factor genes for efficient genotyping applications and trait association mapping. DNA Res **20:** 355–374

Kujur A, Bajaj D, Upadhyaya HD, Das S, Ranjan R, Shree T, Saxena MS, Badoni S, Kumar V, Tripathi S, et al (2015a) A genome-wide SNP scan accelerates trait-regulatory genomic loci identification in chickpea. Sci Rep **5:** 11166

Kujur A, Bajaj D, Upadhyaya HD, Das S, Ranjan R, Shree T, Saxena MS, Badoni S, Kumar V, Tripathi S, et al (2015b) Employing genome-wide SNP discovery and genotyping strategy to extrapolate the natural allelic diversity and domestication patterns in chickpea. Front Plant Sci **6:** 162

Kujur A, Upadhyaya HD, Shree T, Bajaj D, Das S, Saxena MS, Badoni S, Kumar V, Tripathi S, Gowda CLL, et al (2015c) Ultra-high density intra-specific genetic linkage maps accelerate identification of functionally relevant molecular tags governing important agronomic traits in chickpea. Sci Rep **5:** 9468

Kujur A, Upadhyaya HD, Bajaj D, Gowda CL, Sharma S, Tyagi AK, Parida SK (2016) Identification of candidate genes and natural allelic variants for QTLs governing plant height in chickpea. Sci Rep **6:** 27968

Kumar V, Singh A, Mithra SV, Krishnamurthy SL, Parida SK, Jain S, Tiwari KK, Kumar P, Rao AR, Sharma SK, et al (2015) Genome-wide association mapping of salinity tolerance in rice (*Oryza sativa*). DNA Res **22:** 133–145

Lam HM, Xu X, Liu X, Chen W, Yang G, Wong FL, Li MW, He W, Qin N, Wang B, et al (2010) Resequencing of 31 wild and cultivated soybean genomes identifies patterns of genetic diversity and selection. Nat Genet **42:** 1053–1059

Li N, Li Y (2015) Maternal control of seed size in plants. J Exp Bot **66:** 1087–1097

Li N, Li Y (2016) Signaling pathways of seed size control in plants. Curr Opin Plant Biol **33:** 23–32

Li Y, Fan C, Xing Y, Yun P, Luo L, Yan B, Peng B, Xie W, Wang G, Li X, et al (2014) *Chalk5* encodes a vacuolar H⁺-translocating pyrophosphatase influencing grain chalkiness in rice. Nat Genet **46:** 398–404

Li ZS, Szczypka M, Lu YP, Thiele DJ, Rea PA (1996) The yeast cadmium factor protein (YCF1) is a vacuolar glutathione s-conjugate pump. J Biol Chem **271:** 6509–6517

Lipka AE, Tian F, Wang Q, Peiffer J, Li M, Bradbury PJ, Gore MA, Buckler ES, Zhang Z (2012) GAPIT: Genome association and prediction integrated tool. Bioinformatics **28:** 2397–2399

Liu K, Muse SV (2005) PowerMarker: An integrated analysis environment for genetic marker analysis. Bioinformatics **21:** 2128–2129

Lu YP, Li ZS, Drozdowicz YM, Hortensteiner S, Martinoia E, Rea PA (1998) AtMRP2, an Arabidopsis ATP binding cassette transporter able to transport glutathione s-conjugates and chlorophyll catabolites: Functional comparisons with Atmrp1. Plant Cell **10:** 267–282

Malik N, Dwivedi N, Singh AK, Parida SK, Agarwal P, Thakur JK, Tyagi AK (2016) An integrated genomic strategy delineates candidate mediator genes regulating grain size and weight in rice. Sci Rep **6:** 23253

Mather KA, Caicedo AL, Polato NR, Olsen KM, McCouch S, Purugganan MD (2007) The extent of linkage disequilibrium in rice (*Oryza sativa* L.). Genetics **177:** 2223–2232

Moore S, Spackman DH, Stein WH (1958) Chromatography of amino acids on sulfonated polystyrene resins. An improved system. Anal Chem **30:** 1185–1190

Nei M, Tajima F, Tateno Y (1983) Accuracy of estimated phylogenetic trees from molecular data. II. Gene frequency data. J Mol Evol **19:** 153–170

Noctor G, Mhamdi A, Chaouch S, Han Y, Neukermans J, Marquez-Garcia B, Queval G, Foyer CH (2012) Glutathione in plants: An integrated overview. Plant Cell Environ **35:** 454–484

Ohkama-Ohtsu N, Radwan S, Peterson A, Zhao P, Badr AF, Xiang C, Oliver DJ (2007) Characterization of the extracellular γ-glutamyl transpeptidases, GGT1 and GGT2, in *Arabidopsis*. Plant J **49:** 865–877

Okoronkwo NE, Mba KC, Nnorom IC (2017) Estimation of protein content and amino acid compositions in selected plant samples using UV-Vis spectrophotometric method. Am J Food Sci Health **3:** 41–46

Orsi CH, Tanksley SD (2009) Natural variation in an ABC transporter gene associated with seed size evolution in tomato species. PLoS Genet **5:** e1000347

Panzeri D, Cassani E, Doria E, Tagliabue G, Forti L, Campion B, Bollini R, Brearley CA, Pilu R, Nielsen E, et al (2011) A defective ABC transporter of the MRP family, responsible for the bean *lpa1* mutation, affects the regulation of the phytic acid pathway, reduces seed myo-inositol and alters ABA sensitivity. New Phytol **191:** 70–83

Parween S, Nawaz K, Roy R, Pole AK, Venkata Suresh B, Misra G, Jain M, Yadav G, Parida SK, Tyagi AK, et al (2015) An advanced draft genome assembly of a *desi* type chickpea (*Cicer arietinum* L.). Sci Rep **5:** 12806

Pritchard JK, Stephens M, Donnelly P (2000) Inference of population structure using multilocus genotype data. Genetics **155:** 945–959

Purcell S, Neale B, Todd-Brown K, Thomas L, Ferreira MA, Bender D, Maller J, Sklar P, de Bakker PI, Daly MJ, et al (2007) PLINK: A tool set for whole-genome association and population-based linkage analyses. Am J Hum Genet **81:** 559–575

Riedelsheimer C, Lisec J, Czedik-Eysenberg A, Sulpice R, Flis A, Grieder C, Altmann T, Stitt M, Willmitzer L, Melchinger AE (2012) Genome-wide association mapping of leaf metabolic profiles for dissecting complex traits in maize. Proc Natl Acad Sci USA **109:** 8872–8877

Sakiroglu M, Sherman-Broyles S, Story A, Moore KJ, Doyle JJ, Charles Brummer E (2012) Patterns of linkage disequilibrium and association mapping in diploid alfalfa (*M. sativa* L.). Theor Appl Genet **125:** 577–590

Saxena MS, Bajaj D, Das S, Kujur A, Kumar V, Singh M, Bansal KC, Tyagi AK, Parida SK (2014a) An integrated genomic approach for rapid delineation of candidate genes regulating agro-morphological traits in chickpea. DNA Res **21:** 695–710

Saxena MS, Bajaj D, Kujur A, Das S, Badoni S, Kumar V, Singh M, Bansal KC, Tyagi AK, Parida SK (2014b) Natural allelic diversity, genetic structure and linkage disequilibrium pattern in wild chickpea. PLoS One **9:** e107484

Shi J, Wang H, Schellin K, Li B, Faller M, Stoop JM, Meeley RB, Ertl DS, Ranch JP, Glassman K (2007) Embryo-specific silencing of a transporter reduces phytic acid content of maize and soybean seeds. Nat Biotechnol **25:** 930–937

Singh VK, Khan AW, Jaganathan D, Thudi M, Roorkiwal M, Takagi H, Garg V, Kumar V, Chitikineni A, Gaur PM, et al (2016) QTL-seq for rapid identification of candidate genes for 100-seed weight and root/total plant dry weight ratio under rainfed conditions in chickpea. Plant Biotechnol J **14:** 2110–2119

Song XJ, Kuroha T, Ayano M, Furuta T, Nagai K, Komeda N, Segami S, Miura K, Ogawa D, Kamura T, et al (2015) Rare allele of a previously unidentified histone H4 acetyltransferase enhances grain weight, yield, and plant biomass in rice. Proc Natl Acad Sci USA **112:** 76–81

Srivastava R, Bajaj D, Malik A, Singh M, Parida SK (2016) Transcriptome landscape of perennial wild *Cicer microphyllum* uncovers functionally relevant molecular tags regulating agronomic traits in chickpea. Sci Rep **6:** 33616

Srivastava R, Upadhyaya HD, Kumar R, Daware A, Basu U, Shimray PW, Tripathi S, Bharadwaj C, Tyagi AK, et al (2017) A multiple QTL-Seq strategy delineates potential genomic loci governing flowering time in chickpea. Front Plant Sci **8:** 1105

Tamura K, Dudley J, Nei M, Kumar S (2007) MEGA4: Molecular evolutionary genetics analysis (MEGA) software version 4.0. Mol Biol Evol **24:** 1596–1599

Tommasini R, Vogt E, Fromenteau M, Hörtensteiner S, Matile P, Amrhein N, Martinoia E (1998) An ABC-transporter of *Arabidopsis thaliana* has both glutathione-conjugate and chlorophyll catabolite transport activity. Plant J **13:** 773–780

Upadhyaya HD, Bajaj D, Das S, Saxena MS, Badoni S, Kumar V, Tripathi S, Gowda CLL, Sharma S, Tyagi AK, et al (2015) A genome-scale integrated approach aids in genetic dissection of complex flowering time trait in chickpea. Plant Mol Biol **89:** 403–420

Upadhyaya HD, Bajaj D, Narnoliya L, Das S, Kumar V, Gowda CLL, Sharma S, Tyagi AK, Parida SK (2016) Genome-wide scans for delineation of candidate genes regulating seed-protein content in chickpea. Front Plant Sci **7:** 302

van Ooijen JW (2009) MapQTL 6: Software for the Mapping of Quantitative Trait Loci in Experimental Populations of Diploid Species. Kyazma, Wageningen, The Netherlands

Varma Penmetsa R, Carrasquilla-Garcia N, Bergmann EM, Vance L, Castro B, Kassa MT, Sarma BK, Datta S, Farmer AD, Baek JM, et al (2016) Multiple post-domestication origins of *kabuli* chickpea through allelic variation in a diversification-associated transcription factor. New Phytol **211:** 1440–1451

Varshney RK, Paulo MJ, Grando S, van Eeuwijk FA, Keizer LCP, Guo P, Ceccarelli S, Kilian A, Baum M, Graner A (2012) Genome wide association analyses for drought tolerance related traits in barley (*Hordeum vulgare* L.). Field Crops Res **126:** 171–180

Varshney RK, Song C, Saxena RK, Azam S, Yu S, Sharpe AG, Cannon S, Baek J, Rosen BD, Tar'an B, et al (2013) Draft genome sequence of chickpea (*Cicer arietinum*) provides a resource for trait improvement. Nat Biotechnol **31:** 240–246

Varshney RK, Thudi M, Nayak SN, Gaur PM, Kashiwagi J, Krishnamurthy L, Jaganathan D, Koppolu J, Bohra A, Tripathi S, et al (2014) Genetic dissection of drought tolerance in chickpea (*Cicer arietinum* L.). Theor Appl Genet **127:** 445–462

Verma S, Gupta S, Bandhiwal N, Kumar T, Bharadwaj C, Bhatia S (2015) High-density linkage map construction and mapping of seed trait QTLs in chickpea (*Cicer arietinum* L.) using Genotyping-by-Sequencing (GBS). Sci Rep **5:** 17512

Voorrips RE (2002) MapChart: Software for the graphical presentation of linkage maps and QTLs. J Hered **93:** 77–78

Walter S, Kahla A, Arunachalam C, Perochon A, Khan MR, Scofield SR, Doohan FM (2015) A wheat ABC transporter contributes to both grain formation and mycotoxin tolerance. J Exp Bot **66:** 2583–2593

Xiao Y, Cai D, Yang W, Ye W, Younas M, Wu J, Liu K (2012) Genetic structure and linkage disequilibrium pattern of a rapeseed (*Brassica napus* L.) association mapping panel revealed by microsatellites. Theor Appl Genet **125:** 437–447

Yano K, Yamamoto E, Aya K, Takeuchi H, Lo PC, Hu L, Yamasaki M, Yoshida S, Kitano H, Hirano K, et al (2016) Genome-wide association study using whole-genome sequencing rapidly identifies new genes influencing agronomic traits in rice. Nat Genet **48:** 927–934

Zhang Z, Ersoz E, Lai CQ, Todhunter RJ, Tiwari HK, Gore MA, Bradbury PJ, Yu J, Arnett DK, Ordovas JM, et al (2010) Mixed linear model approach adapted for genome-wide association studies. Nat Genet **42:** 355–360

Zhao K, Tung CW, Eizenga GC, Wright MH, Ali ML, Price AH, Norton GJ, Islam MR, Reynolds A, Mezey J, et al (2011) Genome-wide association mapping reveals a rich genetic architecture of complex traits in *Oryza sativa*. Nat Commun **2:** 467

275